contribute to a breakthrough in the establishment of a robust cell culture system of HCVser.

In this study, we demonstrated that PIDR is able to internalize HCV in a receptor-independent manner and provides a clue toward the development of a cell culture system of HCVser in the presence of neutralization antibodies. PIDR may also be useful for the study of viruses that are difficult to internalize into cells due to their low viral titers or the presence of neutralizing antibodies.

Acknowledgments

We thank H. Murase for secretarial work.

This research was supported in part by grants-in-aid from the Ministry of Health, Labor, and Welfare, and the Ministry of Education, Culture, Sports, Science, and Technology, Japan.

References

[1] L.-B. Seeff, Natural history of chronic hepatitis C, Hepatology 36 (2002) S35–S46.

[2] M.-P. Manns, J.-G. McHutchison, S.-C. Gordon, V.-K. Rustgi, M. Shiffman, R. Reindollar, Z.-D. Goodman, K. Koury, M. Ling, J.-K. Albrecht, Peginterferon alfa-2b plus ribavirin compared with interferon alfa-2b plus ribavirin for initial treatment of chronic hepatitis C: a randomised trial, Lancet 358 (2001) 958–965.

[3] J.-M. Pawlotsky, S. Chevaliez, J.-G. McHutchison, The hepatitis C virus life cycle as a target for new antiviral therapies, Gastroenterology 132 (2007) 1979–1998.

[4] T. Wakita, T. Pietschmann, T. Kato, T. Date, M. Miyamoto, Z. Zhao, K. Murthy, A. Habermann, H.-G. Krausslich, M. Mizokami, R. Bartenschlager, T. Jake-Liang, Production of infectious hepatitis C virus in tissue culture from a cloned viral genome, Nat. Med. 11 (2005) 791–796.

[5] N. Hiraga, M. Imamura, M. Tsuge, C. Noguchi, S. Takahashi, E. Iwao, Y. Fujimoto, H. Abe, T. Maekawa, H. Ochi, C. Tateno, K. Yoshizawa, A. Sakai, Y. Sakai, M. Honda, S. Kaneko, T. Wakita, K. Chayama, Infection of human hepatocyte chimeric mouse with genetically engineered hepatitis C virus and its susceptibility to interferon, FEBS Lett. 581 (2007) 1983–1987.

[6] S. Molina, V. Castet, L. Pichard-Garcia, C. Wychowski, E. Meurs, J.-M. Pascussi, C. Sureau, J.-M. Fabre, A. SaCunha, D. Larrey, J. Dubuisson, J. Coste, J. McKeating, P. Maurel, C. Fournier-Wirth, Serum-derived hepatitis C virus infection of primary human hepatocytes is tetraspanin CD81 dependent, J. Virol. 82 (2008) 569–574.

[7] H.-H. Aly, Y. Qi, K. Atsuzawa, N. Usuda, Y. Takada, M. Mizokami, K. Shimotohno, M. Hijikata, Strain-dependent viral dynamics and virus-cell interactions in a novel in vitro system supporting the life cycle of blood-borne hepatitis C virus, Hepatology 50 (2009) 689–696.

[8] A. Ploss, S.-R. Khetani, C.-T. Jones, A.-J. Syder, K. Trehan, V.-A. Gaysinskaya, K. Mu, K. Ritola, C.-M. Rice, S.-N. Bhatia, Persistent hepatitis C virus infection in microscale primary human hepatocyte cultures, Proc. Natl. Acad. Sci. U. S. A 107 (2010) 3141–3145.

[9] D.-R. Burton, Antibodies, viruses and vaccines, Nat. Rev. Immunol. 2 (2002) 706–713.

[10] R. Sobesky, C. Feray, F. Rimlinger, N. Derian, A. Dos Santos, A.-M. Roque-Afonso, D. Samuel, C. Brechot, V. Thiers, Distinct hepatitis C virus core and F protein quasispecies in tumoral and nontumoral hepatocytes isolated via microdissection, Hepatology 46 (2007) 1704–1712.

[11] A. Ploss, M.-J. Evans, V.-A. Gaysinskaya, M. Panis, H. You, Y.-P. de Jong, C.-M. Rice, Human occludin is a hepatitis C virus entry factor required for infection of mouse cells, Nature 457 (2009) 882–886.

[12] N. Landazuri, J.-M. Le Doux, Complexation of retroviruses with charged polymers enhances gene transfer by increasing the rate that viruses are delivered to cells, J. Gene Med. 6 (2004) 1304–1319.

[13] U. O'Doherty, W.-J. Swiggard, M.-H. Malim, Human immunodeficiency virus type 1 spinoculation enhances infection through virus binding, J. Virol. 74 (2000) 10074–10080.

[14] R. Watanabe, S. Matsuyama, F. Taguchi, Receptor-independent infection of murine coronavirus: analysis by spinoculation, J. Virol. 80 (2006) 4901–4908.

[15] L. Ye, X. Wang, S. Wang, G. Luo, Y. Wang, H. Liang, W. Ho, Centrifugal enhancement of hepatitis C virus infection of human hepatocytes, J. Virol. Methods 148 (2008) 161–165.

[16] I. Benedicto, F. Molina-Jimenez, B. Bartosch, F.-L. Cosset, D. Lavillette, J. Prieto, R. Moreno-Otero, A. Valenzuela-Fernandez, R. Aldabe, M. Lopez-Cabrera, The tight junction-associated protein occludin is required for a postbinding step in hepatitis C virus entry and infection, J. Virol. 83 (2009) 8012–8020.

[17] C.-O. Weill, S. Biri, A. Adib, P. Erbacher, A practical approach for intracellular protein delivery, Cytotechnology 56 (2008) 41–48.

[18] T. Okamoto, H. Omori, Y. Kaname, T. Abe, Y. Nishimura, T. Suzuki, T. Miyamura, T. Yoshimori, K. Moriishi, Y. Matsuura, A single-amino-acid mutation in hepatitis C virus NS5A disrupting FKBP8 interaction impairs viral replication, J. Virol. 82 (2008) 3480–3489.

[19] H. Tani, Y. Komoda, E. Matsuo, K. Suzuki, I. Hamamoto, T. Yamashita, K. Moriishi, K. Fujiyama, T. Kanto, N. Hayashi, A. Owsianka, A.-H. Patel, M.-H. Whitt, Y. Matsuura, Replication-competent recombinant vesicular stomatitis virus encoding hepatitis C virus envelope proteins, J. Virol. 81 (2007) 8601–8612.

[20] H.-H. Aly, K. Watashi, M. Hijikata, H. Kaneko, Y. Takada, H. Egawa, S. Uemoto, K. Shimotohno, Serum-derived hepatitis C virus infectivity in interferon regulatory factor-7-suppressed human primary hepatocytes, J. Hepatol. 46 (2007) 26–36.

[21] J. Zhong, P. Gastaminza, G. Cheng, S. Kapadia, T. Kato, D.-R. Burton, S.-F. Wieland, S.-L. Uprichard, T. Wakita, F.-V. Chisari, Robust hepatitis C virus infection in vitro, Proc. Natl. Acad. Sci. U. S. A 102 (2005) 9294–9299.

[22] T. Morris, B. Robertson, M. Gallagher, Rapid reverse transcription-PCR detection of hepatitis C virus RNA in serum by using the TaqMan fluorogenic detection system, J. Clin. Microbiol. 34 (1996) 2933–2936.

[23] R.F. Clayton, A. Owsianska, J. Aitken, S. Graham, D. Bhella, A.H. Patel, Analysis of antigenicity and topology of E2 glycoprotein present on recombinant hepatitis C virus-like particles, J. Virol. 76 (2002) 7672–7682.

[24] P. Pileri, Y. Uematsu, S. Campagnoli, G. Galli, F. Falugi, R. Petracca, A.-J. Weiner, M. Houghton, D. Rosa, G. Grandi, S. Abrignani, Binding of hepatitis C virus to CD81, Science 282 (1998) 938–941.

[25] D. Lavillette, Y. Morice, G. Germanidis, P. Donot, A. Soulier, E. Pagkalos, G. Sakellariou, L. Intrator, B. Bartosch, J.-M. Pawlotsky, F.-L. Cosset, Human serum facilitates hepatitis C virus infection, and neutralizing responses inversely correlate with viral replication kinetics at the acute phase of hepatitis C virus infection, J. Virol. 79 (2005) 6023–6034.

[26] Z. Stamataki, C. Shannon-Lowe, J. Shaw, D. Mutimer, A.-B. Rickinson, J. Gordon, D.-H. Adams, P. Balfe, J.-A. McKeating, Hepatitis C virus association with peripheral blood B lymphocytes potentiates viral infection of liver-derived hepatoma cells, Blood 113 (2009) 585–593.

[27] E. Scarselli, H. Ansuini, R. Cerino, R.-M. Roccasecca, S. Acali, G. Filocamo, C. Traboni, A. Nicosia, R. Cortese, A. Vitelli, The human scavenger receptor class B type I is a novel candidate receptor for the hepatitis C virus, EMBO. J. 21 (2002) 5017–5025.

[28] M.-J. Evans, T. von Hahn, D.-M. Tscherne, A.-J. Syder, M. Panis, B. Wolk, T. Hatziioannou, J.-A. McKeating, P.-D. Bieniasz, C.-M. Rice, Claudin-1 is a hepatitis C virus co-receptor required for a late step in entry, Nature 446 (2007) 801–805.

[29] J.-T. Blackard, N. Kemmer, K.-E. Sherman, Extrahepatic replication of HCV: insights into clinical manifestations and biological consequences, Hepatology 44 (2006) 15–22.

[30] T. Kato, T. Date, M. Miyamoto, A. Furusaka, K. Tokushige, M. Mizokami, T. Wakita, Efficient replication of the genotype 2a hepatitis C virus subgenomic replicon, Gastroenterology 125 (2003) 1808–1817.

[31] H. Aizaki, S. Nagamori, M. Matsuda, H. Kawakami, O. Hashimoto, H. Ishiko, M. Kawada, T. Matsuura, S. Hasumura, Y. Matsuura, T. Suzuki, T. Miyamura, Production and release of infectious hepatitis C virus from human liver cell cultures in the three-dimensional radial-flow bioreactor, Virology 314 (2003) 16–25.

nature immunology

The IκB kinase complex regulates the stability of cytokine-encoding mRNA induced by TLR–IL-1R by controlling degradation of regnase-1

Hidenori Iwasaki[1,2], Osamu Takeuchi[1,3], Shunsuke Teraguchi[1,4], Kazufumi Matsushita[1,6], Takuya Uehata[1,5], Kanako Kuniyoshi[1,3], Takashi Satoh[1], Tatsuya Saitoh[1,3], Mutsuyoshi Matsushita[2], Daron M Standley[4] & Shizuo Akira[1,3]

Toll-like receptor (TLR) signaling activates the inhibitor of transcription factor NF-κB (IκB) kinase (IKK) complex, which governs NF-κB-mediated transcription during inflammation. The RNase regnase-1 serves a critical role in preventing autoimmunity by controlling the stability of mRNAs that encode cytokines. Here we show that the IKK complex controlled the stability of mRNA for interleukin 6 (IL-6) by phosphorylating regnase-1 in response to stimulation via the IL-1 receptor (IL-1R) or TLR. Phosphorylated regnase-1 underwent ubiquitination and degradation. Regnase-1 was reexpressed in IL-1R- or TLR-activated cells after a period of lower expression. Regnase-1 mRNA was negatively regulated by regnase-1 itself via a stem-loop region present in the regnase-1 3′ untranslated region. Our data demonstrate that the IKK complex phosphorylates not only IκBα, thereby activating transcription, but also regnase-1, thereby releasing a 'brake' on IL-6 mRNA expression.

Inflammatory responses are rapidly elicited in response to infection by various pathogens and cellular stimuli[1–3]. Inflammation is mediated by proinflammatory cytokines such as tumor necrosis factor (TNF), interleukin 1β (IL-1β) and IL-6. Expression of cytokines is suppressed in resting cells of the innate immune system, whereas it is rapidly induced in response to infection by pathogens via a set of pattern-recognition receptors, such as Toll-like receptors (TLRs), helicase RIG-I–like receptors and biosensor Nod–like receptors.

The cytoplasmic portion of TLRs, the Toll–IL-1R domain, is homologous to that of the IL-1 receptor (IL-1R)[4]. IL-1R and all TLRs except TLR3 trigger intracellular signaling pathways by recruiting the adaptor MyD88. IL-1R-associated kinase 4 (IRAK4) then associates with MyD88 and activates IRAK1 and IRAK2 (ref. 5). The IRAKs then dissociate from MyD88 and interact with TRAF6, which acts as an E3 ubiquitin protein ligase[6]. Together with an E2 ubiquitin-conjugating enzyme complex composed of Ubc13 and Uev1A, TRAF6 catalyzes the formation of a lysine 63 (K63)-linked polyubiquitin chain on TRAF6 itself as well as the generation of an unconjugated free polyubiquitin chain[7]. A complex of the kinase TAK1 and the TAK1-binding proteins TAB1, TAB2 and TAB3 is activated by the unconjugated free K63 polyubiquitin chain and phosphorylates inhibitor of transcription factor NF-κB (IκB) kinase-β (IKKβ) and mitogen-activated protein kinase (MAP) kinase kinase 6 (ref. 6). In addition, linear ubiquitination of the NF-κB modulator IKKγ (NEMO) by a linear ubiquitin-chain assembly complex composed of HOIP, HOIL-1L and SHARPIN is required for activation of NF-κB[8–10]. Subsequently, the IKK complex, composed of IKKα, IKKβ and NEMO, phosphorylates the NF-κB-inhibitory protein IκBα on a DSGXXS motif (where 'X' is any amino acid)[11,12]. Phosphorylated IκBα undergoes ubiquitination by the the E3 ligase β-TrCP complex (β-transducin repeat–containing protein; also known as FBW1) and is degraded by the proteasome system, which thereby frees NF-κB to translocate to the nucleus and activate the transcription of genes encoding proinflammatory cytokines[11–15]. Activation of the MAP kinase cascade is responsible for the formation of another transcription factor complex, AP-1, that targets genes encoding cytokines. Signaling via the TNF receptor (TNFR) also leads to the activation of NF-κB by ubiquitination of the kinase RIP1, followed by activation of the TAK1 complex and linear ubiquitination of NEMO[8,16,17].

In addition to being controlled by transcriptional activation, cytokine-encoding mRNAs are controlled at the level of mRNA itself[18]. Proinflammatory cytokine–encoding mRNAs tend to have short half-lives, and mRNA stability is important for controlling the strength and duration of inflammation[19]. For example, tristetraprolin associates with AU-rich elements present in the 3′ untranslated regions (UTRs) of TNF mRNA and destabilizes TNF mRNA[20,21]. The cytoplasmic protein encoded by *Zc3h12a* is composed of a PIN-like

[1]Laboratory of Host Defense, World Premier International Immunology Frontier Research Center, Osaka University, Osaka, Japan. [2]Central Pharmaceutical Research Institute, Japan Tobacco, Osaka, Japan. [3]Research Institute for Microbial Diseases, Osaka University, Osaka, Japan. [4]Laboratory of Systems Immunology, World Premier International Immunology Frontier Research Center, Osaka University, Osaka, Japan. [5]Department of Geriatric Medicine and Nephrology, Osaka University Graduate School of Medicine, Osaka, Japan. [6]Present address: Laboratory of Allergic Diseases, Institute for Advanced Medical Sciences, Hyogo College of Medicine, Hyogo, Japan. Correspondence should be addressed to O.T. (otake@biken.osaka-u.ac.jp) or S.A. (sakira@biken.osaka-u.ac.jp).

Received 20 May; accepted 15 September; published online 30 October 2011; doi:10.1038/ni.2137

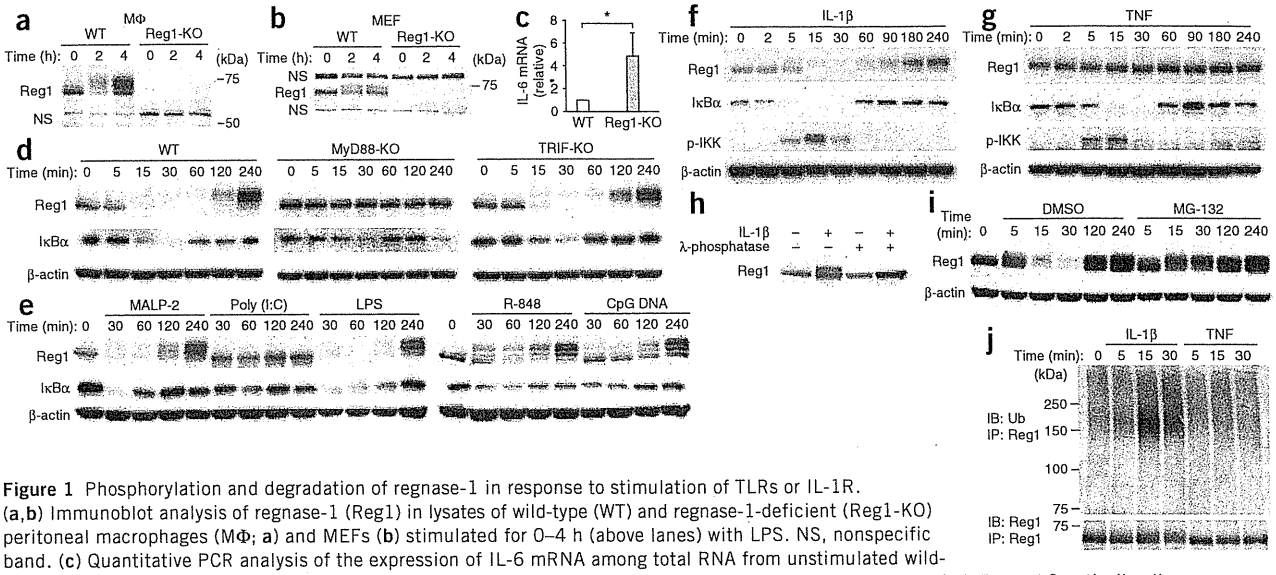

Figure 1 Phosphorylation and degradation of regnase-1 in response to stimulation of TLRs or IL-1R. (**a**,**b**) Immunoblot analysis of regnase-1 (Reg1) in lysates of wild-type (WT) and regnase-1-deficient (Reg1-KO) peritoneal macrophages (MΦ; **a**) and MEFs (**b**) stimulated for 0–4 h (above lanes) with LPS. NS, nonspecific band. (**c**) Quantitative PCR analysis of the expression of IL-6 mRNA among total RNA from unstimulated wild-type and regnase-1-deficient macrophages .*$P < 0.05$ (Student's *t*-test). (**d**) Immunoblot analysis of regnase-1, IκBα and β-actin (loading control) in wild-type, MyD88-deficient (MyD88-KO) and TRIF-deficient (TRIF-KO) macrophages stimulated for 0–240 min (above lanes) with LPS. (**e**) Immunoblot analysis of regnase-1, IκBα and β-actin in lysates of wild-type peritoneal macrophages stimulated for 0–240 min (above lanes) with MALP-2 (10 ng/ml), poly(I:C) (100 μg/ml), LPS (100 ng/ml), R-848 (10 nM) or CpG DNA (1 μM). (**f**,**g**) Immunoblot analysis of regnase-1, IκBα, phosphorylated (p-) IKK and β-actin in HeLa cells stimulated for 0–240 min (above lanes) with IL-1β (10 ng/ml; **f**) or TNF (10 ng/ml; **g**). (**h**) Immunoblot analysis of regnase-1 in HeLa cell lysates left unstimulated (–) or stimulated (+) with IL-1β and left untreated (–) or treated (+) with λ-phosphatase. (**i**) Immunoblot analysis of regnase-1 in HeLa cells pretreated with 0.1% dimethyl sulfoxide (DMSO) or the proteasome inhibitor MG-132 (1 μM), then stimulated for 0–240 min (above lanes) with IL-1β. (**j**) Immunoassay of lysates of HeLa cells stimulated for 0–30 min (above lanes) with IL-1β or TNF, followed by immunoprecipitation (IP) with anti-regnase-1 and immunoblot analysis (IB) with antibody to ubiquitin (Ub) or Reg1. Data are representative of three to five independent experiments (error bars (**c**), s.d.).

RNase domain and a CCCH-type zinc-finger domain[22]. As its RNase activity is directly responsible for regulating cytokine mRNA abundance, we have called this protein regulatory RNase 1 (regnase-1). The production of IL-6 and the p40 subunit of IL-12 in response to TLR ligands is much greater in regnase-1-deficient (*Zc3h12a*$^{-/-}$) macrophages[22]. The decay of IL-6 mRNA is impaired in regnase-1-deficient macrophages, and regnase-1 destabilizes mRNA via a conserved element independently of AU-rich elements present in the 3′ UTR of IL-6. Regnase-1-deficient mice spontaneously develop severe autoimmune inflammatory disease, which indicates that regnase-1-mediated control of mRNA expression has an essential role in maintaining homeostasis.

Although expression of regnase-1 mRNA is induced in response to stimulation with TLR ligands, the regulation of regnase-1 protein during the course of inflammation has not been clarified. In this study, we found that regnase-1 was rapidly degraded in response to stimulation with IL-1β or TLR ligands but not in response to TNF. Degradation of regnase-1 protein was important for higher expression of IL-6 mRNA. We identified IKKα,β as the kinase that induced ubiquitin-proteasome-mediated degradation of regnase-1 via β-TrCP. Regnase-1 mRNA was reexpressed about 240 min after stimulation of the TLR or IL-1R. Regnase-1 mRNA was targeted for degradation by regnase-1 protein. We generated a mathematical model in which the IKK complex phosphorylates not only IκBα, thereby activating transcription of genes encoding cytokines, but also regnase-1, thereby releasing the 'brake' on IL-6 mRNA expression. Moreover, as expression of the gene encoding regnase-1 was regulated by NF-κB, regnase-1 effectively functions as a 'molecular timer' that allows rapid generation of IL-6 mRNA during acute inflammation but inhibits sustained IL-6 production.

RESULTS

Modification of regnase-1 in response to TLR or IL-1R stimulation

To examine the expression of regnase-1 protein, we did immunoblot analysis of thioglycollate-elicited peritoneal macrophages and mouse embryonic fibroblasts (MEFs) from wild-type and regnase-1-deficient (*Zc3h12a*$^{-/-}$) mice. We confirmed the lack of regnase-1 expression in regnase-1-deficient peritoneal macrophages and MEFs (**Fig. 1a,b**). Notably, regnase-1 protein was expressed even in unstimulated macrophages and MEFs. In addition, regnase-1 protein was expressed in mouse thymus, spleen, lymph nodes and lungs (**Supplementary Fig. 1**). IL-6 mRNA was fivefold more abundant in regnase-1-deficient macrophages than wild-type macrophages even without stimulation (**Fig. 1c**), which suggested that expression of regnase-1 protein in unstimulated cells was required for the suppression of subtle inflammatory reactions. That hypothesis is consistent with the observed spontaneous development of autoimmune disease in regnase-1-deficient mice. When we looked closely at changes in regnase-1 expression, we found that the mobility of regnase-1 protein changed rapidly in response to lipopolysaccharide (LPS) and disappeared within 15 min of stimulation (**Fig. 1d**). Subsequently, regnase-1 reappeared within 120 min of stimulation, although most regnase-1 protein migrated slowly in the gel, which indicated that regnase-1 underwent some form of modification. It is well known that stimulation via TLR or IL-1β induces rapid degradation of IκBα protein and is followed by re-expression, which allows the nuclear translocation of NF-κB[14,15]. The kinetics of the LPS-induced regnase-1 expression was similar to that of IκBα in wild-type macrophages and MEFs (**Fig. 1d** and **Supplementary Fig. 2**). LPS is recognized by TLR4 and triggers distinct signaling pathways via the adaptors MyD88 and TRIF[4]. Both MyD88-dependent and TRIF-dependent pathways are

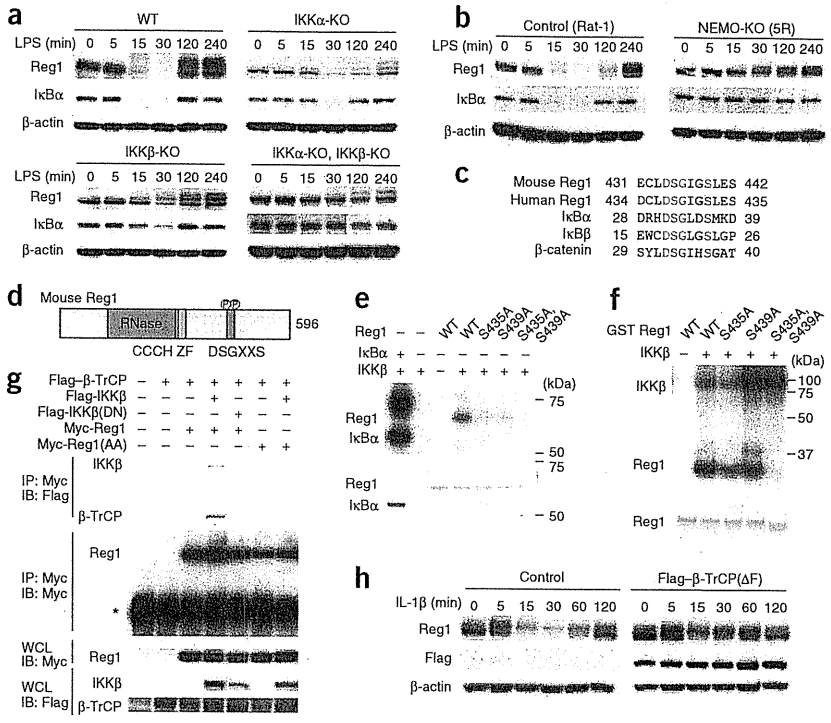

Figure 2 The IKK complex is essential for regnase-1 phosphorylation. (**a**,**b**) Immunoblot analysis of regnase-1, IκBα and β-actin in MEFs from wild-type mice or mice deficient in IKKα (IKKα-KO), IKKβ (IKKβ-KO) or both IKKα and IKKβ (IKKα-KO,IKKβ-KO; **a**) and of Rat-1 (NEMO-sufficient) cells and 5R (NEMO-deficient) cells (**b**), stimulated for 0–240 min (above lanes) with LPS. (**c**) Alignment of DSGXXS motifs (red) in mouse and human regnase-1 and mouse IκBα, IκBβ and β-catenin. (**d**) Regnase-1 domains, including the RNase domain (green), the zinc-finger domain (CCCH ZF; orange) and the DSGXXS domain (red; 596 (far right) indicates total amino acids present). (**e**,**f**) *In vitro* kinase assay (top) of recombinant IKKβ and wild-type or mutant regnase-1 (**e**) or GST fusion proteins of wild-type or mutant regnase-1 (**f**), and SDS-PAGE and Coomassie blue staining (bottom) of wild-type and mutant regnase-1 (all corresponding to regnase-1 amino acids 430–441). kDa, kilodaltons. (**g**) Immunoassay of the association of regnase-1 and β-TrCP in HEK293 cells transfected with various combinations (above lanes) of expression plasmids for Flag-tagged β-TrCP (Flag–β-TrCP), wild-type IKKβ (Flag-IKKβ) or kinase-inactive IKKβ (Flag-IKKβ(DN)), and Myc-tagged wild-type regnase-1 (Myc-Reg1) or S435A,S439A mutant regnase-1 (Myc-Reg1(AA)), followed by immunoprecipitation of proteins from lysates with anti-Myc and immunoblot analysis with anti-Flag or anti-Myc. *, immunoglobulin heavy chain. Below, immunoblot analysis of whole-cell lysates (WCL) with anti-Myc or anti-Flag. (**h**) Immunoblot analysis of regnase-1, dominant negative β-TrCP(ΔF) and β-actin in HeLa cells expressing Flag-tagged β-TrCP(ΔF) or control plasmid and stimulated for 0–120 min (above lanes) with IL-1β. Data are representative of three to four independent experiments.

required for optimal LPS-mediated proinflammatory cytokine production, although each pathway results in the degradation of IκBα and activation of NF-κB[23]. Whereas we observed LPS-induced disappearance of IκBα in MyD88-deficient and TRIF-deficient macrophages, we observed the disappearance of regnase-1 in macrophages from TRIF-deficient mice but not those from MyD88-deficient mice (**Fig. 1d**). Downstream of MyD88, the kinases IRAK1 and IRAK2 or IRAK4 were required for the degradation of regnase-1 in response to LPS (**Supplementary Fig. 3**). In macrophages stimulated with ligands for various TLRs, including MALP-2 (TLR6-TLR2), poly (I:C) (TLR3), LPS (TLR4), R-848 (TLR7) or CpG DNA (TLR9), the modification and disappearance of regnase-1 were induced in response to all TLR ligands except poly (I:C) (**Fig. 1e**). Given that all TLRs except TLR3 signal via MyD88 (ref. 4), these results indicated that the MyD88-dependent signaling pathway was essential for the disappearance in regnase-1 expression. In contrast, stimulation of cells with chemokines and cytokines such as MCP-1, IL-6 and IFN-γ failed to induce changes in regnase-1 expression (**Supplementary Fig. 4**). Consistent with those observations, HeLa human cervical cancer cells stimulated with IL-1β showed modification and disappearance of regnase-1, but those stimulated with TNF did not (**Fig. 1f,g**). In contrast, degradation of IκBα was induced equivalently by IL-1β and TNF. We then investigated the mechanism by which regnase-1 was modified in response to stimulation via TLRs or IL-1R. Treatment of IL-1β-stimulated cell lysates with λ-phosphatase resulted in the disappearance of slowly migrating regnase-1 (**Fig. 1h**), which indicated that regnase-1 was phosphorylated in response to IL-1β. Treatment of HeLa cells with the proteasome inhibitor MG-132 resulted in considerable impairment in the decrease in regnase-1 (**Fig. 1i**), and immunoblot analysis showed that IL-1β induced the ubiquitination of regnase-1 but TNF did not (**Fig. 1j**). Thus, regnase-1 was rapidly phosphorylated in response to IL-1β and was degraded via the ubiquitin-proteasome pathway.

IKKβ can phosphorylate regnase-1 on a DSGXXS motif

We next searched for the kinase responsible for the phosphorylation and degradation of regnase-1. Neither modification nor degradation of regnase-1 was affected by pretreatment of HeLa cells with cycloheximide or actinomycin D (**Supplementary Fig. 5**), which indicated that modification of regnase-1 did not require IL-1β-mediated protein synthesis or gene transcription. Although MAP kinases such as Erk, Jnk and p38, as well as phosphoinositide-3-OH kinases, are activated in response to stimulation via TLRs or IL-1R, pretreatment of HeLa cells with inhibitors of those receptors failed to prevent the IL-1β-induced degradation and reappearance of regnase-1 (**Supplementary Fig. 6**). In contrast, treatment with the IKKβ inhibitor TPCA-1 inhibited the degradation of regnase-1 (**Supplementary Fig. 6**). Therefore, we investigated the contribution of the IKK complex to regnase-1 degradation. MEFs lacking IKKα showed unimpaired regnase-1 degradation in response to LPS, whereas IKKβ-deficient MEFs showed partially impaired degradation of regnase-1 and IκBα (**Fig. 2a**). However, cells lacking both IKKα and IKKβ did not show any degradation of regnase-1 or IκBα in response to LPS (**Fig. 2a**). Nevertheless, slowly migrating regnase-1 still appeared in the late phase of stimulation, which suggested that another kinase phosphorylated regnase-1 without affecting its degradation. Consistent with that, NEMO-deficient Rat-1 rat fibroblasts (5R cells)[24] did not have less regnase-1 or IκBα after LPS stimulation than did control NEMO-sufficient Rat-1 cells (**Fig. 2b**), which indicated that the IKK complex was essential for the degradation of regnase-1. Sequence analysis showed that regnase-1

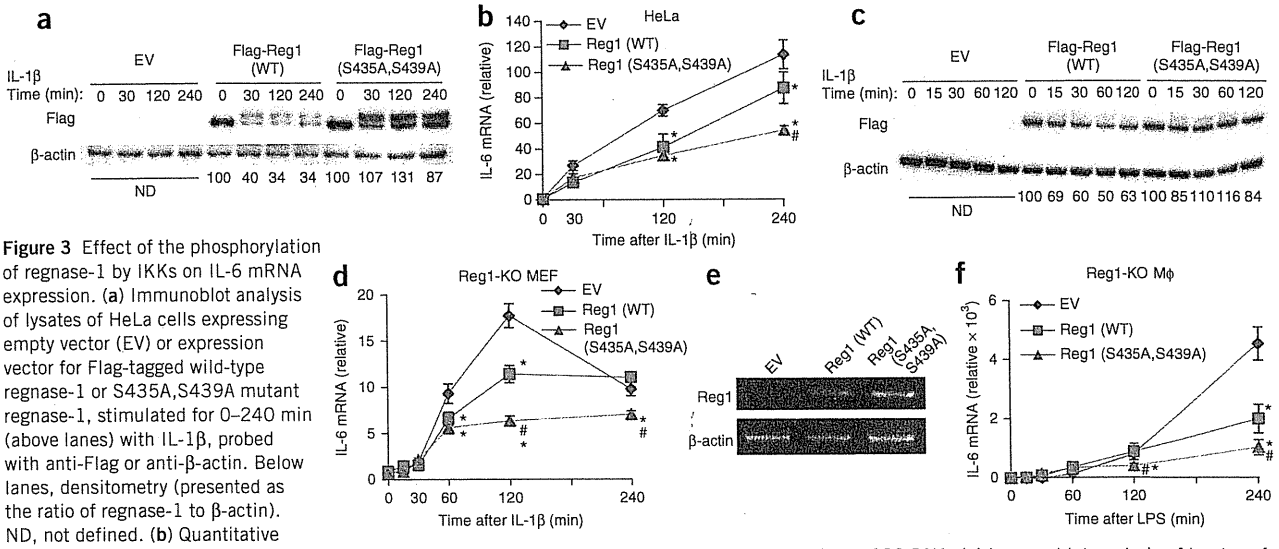

Figure 3 Effect of the phosphorylation of regnase-1 by IKKs on IL-6 mRNA expression. (**a**) Immunoblot analysis of lysates of HeLa cells expressing empty vector (EV) or expression vector for Flag-tagged wild-type regnase-1 or S435A,S439A mutant regnase-1, stimulated for 0–240 min (above lanes) with IL-1β, probed with anti-Flag or anti-β-actin. Below lanes, densitometry (presented as the ratio of regnase-1 to β-actin). ND, not defined. (**b**) Quantitative PCR analysis of the expression of IL-6 mRNA among total RNA from the cells in **a**, presented relative to 18S RNA. (**c**) Immunoblot analysis of lysates of regnase-1-deficient MEFs infected with control retrovirus (EV) or retrovirus expressing Flag-tagged wild-type regnase-1 or the S435A,S439A regnase-1 mutant, then stimulated for 0–120 min (above lanes) with IL-1β, probed with anti-Flag or β-actin. Below lanes, densitometry (as in **a**). (**d**) Quantitative PCR analysis as in **b** of total RNA from the cells in **c**. (**e**) Semiquantitative RT-PCR analysis of wild-type regnase-1 and S435A,S439A mutant regnase-1 in macrophages prepared from regnase-1-deficient bone marrow cells infected with retrovirus as in **c**. (**f**) Quantitative PCR analysis (as in **b**) of the cells in **e**, stimulated for 0–240 min (horizontal axis) with LPS. $*P < 0.05$, empty vector versus regnase-1 (wild type or S435A,S439A), and $P < 0.05$, wild-type regnase-1 versus S435A,S439A regnase-1 (Student's *t*-test). Data are representative of three to four independent experiments with similar results (mean ± s.d. of triplicates in **b**,**d**,**f**).

had the canonical DSGXXS motif known to be phosphorylated by IKKs[11] (**Fig. 2c**). This motif in regnase-1 was located in an unstructured region, C-terminal to the nuclease and CCCH-type zinc-finger domains (**Fig. 2d**), and the motif was conserved among species from zebrafish to humans (**Supplementary Fig. 7**). As expected, IKKβ and IKKα phosphorylated synthesized full-length regnase-1 protein and a glutathione *S*-transferase (GST) fusion peptide corresponding to amino acids 430–441, including the DSGXXS motif, *in vitro* (**Fig. 2e,f** and data not shown). Furthermore, the phosphorylation of mouse regnase-1 was attenuated by the substitution of serine residues Ser435 and Ser439 with alanine (S435A,S439A; **Fig. 2e,f**), which indicated that the two serine residues present in the DSGXXS motif were the targets of the phosphorylation of regnase-1 by IKKs. In addition, coimmunoprecipitation analysis showed that IKKβ interacted with regnase-1 endogenously (**Supplementary Fig. 8a,b**). Stimulation with IL-1β failed to change this interaction, which suggested that regnase-1 formed a stable complex with IKKβ in resting cells. Although the DSGXXS motif is also known to be phosphorylated by another kinase, GSK3β[13], treatment with the GSK3β inhibitor LiCl failed to inhibit IL-1β-mediated degradation of regnase-1 (**Supplementary Fig. 9**). It is well known that the phosphorylated DSGXXS sequence is subsequently recognized by the E3 ligase β-TrCP for polyubiquitination[13]. To determine if regnase-1 interacts with β-TrCP, we expressed β-TrCP and regnase-1 in HEK293 human embryonic kidney cells and found that β-TrCP precipitated together with regnase-1 only when wild-type IKKβ was coexpressed (**Fig. 2g**). In contrast, coexpression of kinase-inactive IKKβ did not induce an association between β-TrCP and regnase-1. Furthermore, mutant regnase-1 (S435A,S439A)

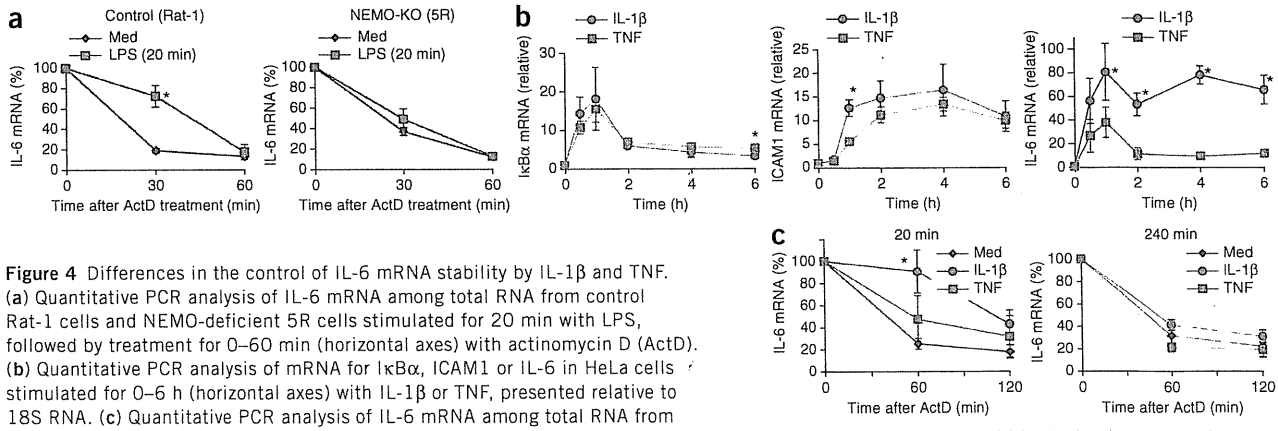

Figure 4 Differences in the control of IL-6 mRNA stability by IL-1β and TNF. (**a**) Quantitative PCR analysis of IL-6 mRNA among total RNA from control Rat-1 cells and NEMO-deficient 5R cells stimulated for 20 min with LPS, followed by treatment for 0–60 min (horizontal axes) with actinomycin D (ActD). (**b**) Quantitative PCR analysis of mRNA for IκBα, ICAM1 or IL-6 in HeLa cells stimulated for 0–6 h (horizontal axes) with IL-1β or TNF, presented relative to 18S RNA. (**c**) Quantitative PCR analysis of IL-6 mRNA among total RNA from HeLa cells stimulated for 20 or 240 min (above plots) with medium alone (Med), IL-1β or TNF, then treated for 0–120 min (horizontal axes) with actinomycin D. $*P < 0.05$ (Student's *t*-test). Data are from three independent experiments (mean ± s.d.).

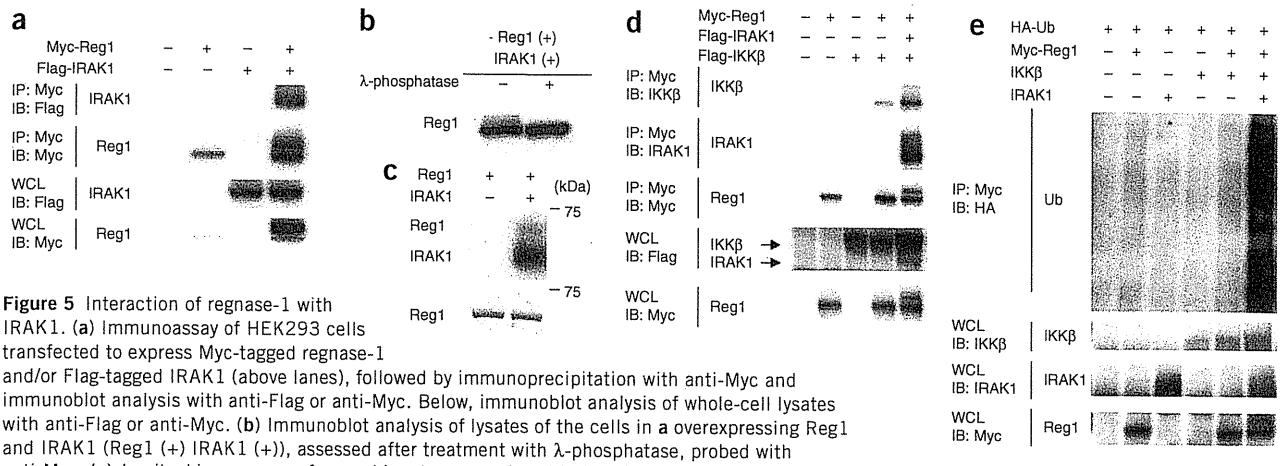

Figure 5 Interaction of regnase-1 with IRAK1. (**a**) Immunoassay of HEK293 cells transfected to express Myc-tagged regnase-1 and/or Flag-tagged IRAK1 (above lanes), followed by immunoprecipitation with anti-Myc and immunoblot analysis with anti-Flag or anti-Myc. Below, immunoblot analysis of whole-cell lysates with anti-Flag or anti-Myc. (**b**) Immunoblot analysis of lysates of the cells in **a** overexpressing Reg1 and IRAK1 (Reg1 (+) IRAK1 (+)), assessed after treatment with λ-phosphatase, probed with anti-Myc. (**c**) *In vitro* kinase assay of recombinant regnase-1 and IRAK1 (top), and SDS-PAGE and Coomassie blue staining of regnase-1 (bottom). (**d**) Immunoassay of HEK293 cells transfected to express Myc-tagged regnase-1 and/or Flag-tagged IRAK1 or IKKβ (above lanes), followed by immunoprecipitation from lysates with anti-Myc and immunoblot analysis with anti-IKKβ, anti-IRAK1 or anti-Myc. Below, immunoblot analysis of whole-cell lysates with anti-Flag or anti-Myc. (**e**) Immunoassay of HEK293 cells transfected to express hemagglutinin-tagged ubiquitin (HA-Ub), Myc-tagged regnase-1 and/or IKKβ or IRAK1 (above lanes), followed by immunoprecipitation from lysates with anti-Myc and immunoblot analysis of ubiquitin (with anti-HA). Below, immunoblot analysis of whole-cell lysates with anti-IKKβ, anti-IRAK1 or anti-Myc. Data are representative of three to four independent experiments.

failed to interact with β-TrCP and IKKβ (**Fig. 2g**), which suggested that phosphorylation of the DSGXXS sequence present in regnase-1 was essential for its interaction with β-TrCP. To evaluate the role of β-TrCP in the degradation of regnase-1, we used a β-TrCP mutant that fails to associate with other subunits of the E3 ubiquitin ligase complex and functions as a dominant-negative form (β-TrCP(ΔF))[25]. Overexpression of β-TrCP(ΔF) in HeLa cells resulted in less IL-1β-mediated degradation of regnase-1 without affecting the phosphorylation (**Fig. 2h**). Collectively, these results indicated that IKKα,β phosphorylated regnase-1 on its canonical DSGXXS sequence and that β-TrCP was responsible for activation of the ubiquitin-proteasome pathway.

Regnase-1 degradation controls IL-6 mRNA expression

IL-6 mRNA is stabilized in regnase-1-deficient macrophages[22]. To examine the role of IKK-mediated phosphorylation and degradation of regnase-1 in controlling the stability of IL-6 mRNA, we expressed wild-type regnase-1 and the S435A,S439A regnase-1 mutant in HeLa ells. Whereas wild-type regnase-1 was degraded in response to IL-1β stimulation, the S435A,S439A mutant was resistant to the stimuli (**Fig. 3a**). Notably, the S435A,S439A mutant protein still migrated slowly after stimulation, which indicated amino acids other than Ser435 and Ser439 were phosphorylated by an unknown kinase without affecting regnase-1 degradation. Although the expression of IL-6 mRNA decreased even when wild-type regnase-1 was expressed, expression of the S435A,S439A mutant suppressed IL-6 mRNA expression more in response to IL-1β (**Fig. 3b**). Next we expressed wild-type regnase-1 and the S435A,S439A mutant via retrovirus in regnase-1-deficient MEFs. Whereas wild-type regnase-1 was degraded in response to IL-1β, the S435A,S439A mutant was resistant to degradation (**Fig. 3c**). Consistent with the results obtained with HeLa cells, the S435A,S439A mutant was more potent in suppressing IL-6 mRNA expression than was wild-type regnase-1 (**Fig. 3d**). Furthermore, wild-type regnase-1 and the S435A,S439A mutant expressed via retrovirus in regnase-1-deficient macrophages acted similarly. Whereas expression of wild-type regnase-1 also partially inhibited IL-6 expression in response to LPS, the S435A,S439A mutant was more potent in suppressing IL-6 mRNA expression (**Fig. 3e,f**). These results indicated that IKK-mediated phosphorylation of regnase-1 was involved in augmenting IL-6 mRNA expression in the course of TLR- or IL-1R-mediated inflammation.

The IKK complex enhances IL-6 mRNA stability

Next we determined if the IKK complex controlled the stability of IL-6 mRNA in addition to controlling transcription. IL-6 mRNA was more stable in wild-type (Rat-1) cells stimulated for 20 min with LPS than in unstimulated cells, and the mRNA half-life was longer (**Fig. 4a**). In contrast, cells lacking NEMO (5R cells) failed to stabilize IL-6 mRNA in response to stimulation for 20 min with LPS (**Fig. 4a**), which indicated that the IKK complex also regulated the stability of cytokine mRNA in addition to controlling transcription. As IL-1β induced degradation of regnase-1 within 15 min, but not TNF did not, we compared the expression of a set of NF-κB-inducible genes in HeLa cells in response to stimulation with IL-1β or TNF. Phosphorylation of IKKs was induced with similar kinetics in response to IL-1β or TNF (**Fig. 1f,g**). Although IL-1β and TNF induced IκBα mRNA and the integrin ligand ICAM1 with similar kinetics, consistent with a published report[19], the expression of IL-6 mRNA was higher in response to IL-1β stimulation (**Fig. 4b**). When we measured the stability of IL-6 mRNA 20 min after stimulation with IL-1β or TNF, we found that IL-1β extended the half-life of IL-6 mRNA much more than TNF did (**Fig. 4c** and **Table 1**). Consistent with the reappearance of regnase-1 protein 60–90 min after stimulation with IL-1β (**Fig. 1f**), the half-life of IL-6 mRNA at 240 min was similar after stimulation with IL-1β or TNF (**Fig. 4c** and **Table 1**), which indicated that the

Table 1 Change in IL-6 mRNA half-life in response to IL-1β stimulation in HeLa cells

Stimulation	20 min	240 min
Medium alone	40.6 ± 3.3	44.6 ± 5.4
IL-1β	110.9 ± 11.6	51.7 ± 4.2
TNF	48.0 ± 4.4	37.4 ± 1.8

Half-life of IL-6 mRNA (in min) in HeLa cells before (Medium alone) or 20 or 240 min after stimulation with IL-1β or TNF (calculated based on the kinetic changes in **Fig. 4c**). Data are from three independent experiments (mean ± s.d.).

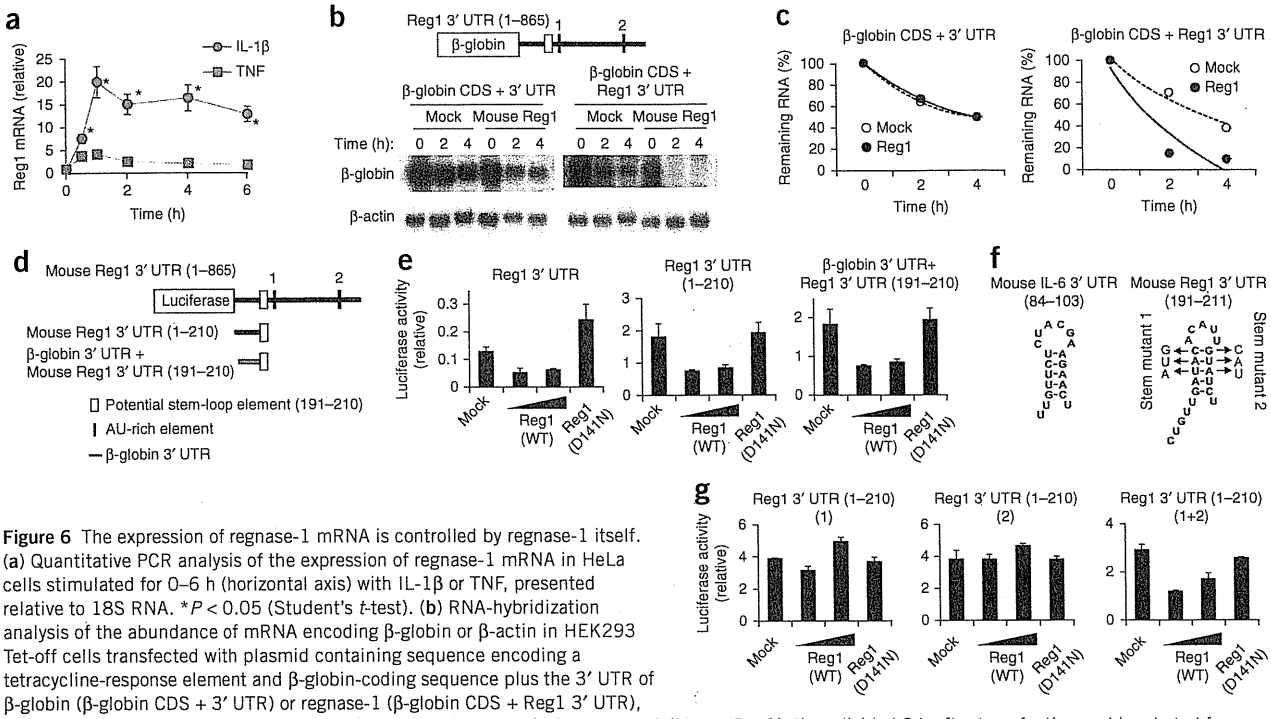

Figure 6 The expression of regnase-1 mRNA is controlled by regnase-1 itself. (**a**) Quantitative PCR analysis of the expression of regnase-1 mRNA in HeLa cells stimulated for 0–6 h (horizontal axis) with IL-1β or TNF, presented relative to 18S RNA. $*P < 0.05$ (Student's *t*-test). (**b**) RNA-hybridization analysis of the abundance of mRNA encoding β-globin or β-actin in HEK293 Tet-off cells transfected with plasmid containing sequence encoding a tetracycline-response element and β-globin-coding sequence plus the 3′ UTR of β-globin (β-globin CDS + 3′ UTR) or regnase-1 (β-globin CDS + Reg1 3′ UTR), together with control empty plasmid (Mock) or expression plasmid for regnase-1 (Mouse Reg1), then divided 3 h after transfection and incubated for an additional 20 h, followed by treatment (time, above lanes) with doxycycline (1 μg/ml). (**c**) Quantification of the autoradiographs in **b**, presented as the ratio of β-globin to β-actin. (**d**) The 3′ UTR of mouse regnase-1 mRNA (positions 1–865) and deletion constructs. (**e**) Luciferase activity of HEK293 cells transfected for 48 h with luciferase reporter plasmids as in **d** (top), together with control plasmid (Mock) or expression plasmid for wild-type regnase-1 or a nuclease-inactive mutant of regnase-1 (D141N); results are presented relative to renilla luciferase activity. (**f**) Predicted stem-loop structure of the regnase-1-responsive element in the 3′ UTR of IL-6 mRNA (left) or regnase-1 mRNA (right), pus mutations leading to disruption of the regnase-1 stem-loop structure (Stem mutant 1 and 2). (**g**) Luciferase activity of HEK293 cells transfected for 48 h with luciferase reporter plasmids containing sequence as in **f** (stem mutants alone (1 or 2) or together (1+2)), together with expression plasmids as in **e** (presented as in **e**). Data are representative of three independent experiments (**a**–**c**) or three independent experiments with similar results (**e**,**g**; error bars, s.d. of duplicates).

kinetics of IL-6 mRNA stability correlated well with the abundance of regnase-1 protein in response to stimulation with IL-1β or TNF. We further investigated the role of regnase-1 degradation in the stability of IL-6 mRNA by comparing the contributions of MyD88 and TRIF in response to LPS. The half-life of IL-6 mRNA was extended in response to LPS in control and TRIF-deficient MEFs (**Supplementary Table 1**). In contrast, LPS did not affect the half-life of IL-6 mRNA in MyD88-deficient cells, consistent with the status of regnase-1 protein expression. These results suggested that the lower abundance of regnase-1 protein in response to simulation with IL-1β or TLR contributed to the greater stability of IL-6 mRNA. Collectively, these results indicated that the IKK complex activated not only the transcription of genes encoding cytokines by the IκBα–NF-κB pathway but also stabilized IL-6 mRNA by degrading regnase-1 in response to stimulation via the IL-1R or TLR (**Supplementary Fig. 10**).

IRAK1 interacts with and phosphorylates regnase-1

We next investigated the mechanism by which regnase-1 was degraded by stimulation with IL-1R or TLR but not by TNFR. The data presented above indicated that activation of the IKK complex alone was not sufficient to induce regnase-1 modification. Whereas signaling molecules downstream of TAK1 are shared by IL-1R, TLR and TNFR, signaling molecules such as MyD88 and IRAKs are activated by IL-1R and TLR but not by TNFR. It has been reported that IRAKs control mRNA stability in addition to activating NF-κB[26,27]. However, cells that lack both IRAK1 and IRAK2 are still able to activate NF-κB downstream of MyD88 (ref. 5). As MyD88, IRAK1 and IRAK2 were all necessary for regnase-1 degradation, the IRAKs degraded regnase-1 by a mechanism independent of simple activation of the IKK complex. Thus, we hypothesized that modification of regnase-1 by IRAKs is necessary for subsequent phosphorylation by the IKKs. When we overexpressed IRAK1 and regnase-1 in HEK293 cells, we observed that IRAK1 precipitated together with regnase-1 (**Fig. 5a**), which indicated that regnase-1 interacted with IRAK1. Further, the mobility of regnase-1 during electrophoresis through the gel changed when IRAK1 was coexpressed (**Fig. 5a**). Treatment of cell lysates with λ-phosphatase resulted in disappearance of regnase-1 protein that migrated more slowly (**Fig. 5b**), which suggested that regnase-1 was phosphorylated by IRAK1. We confirmed that finding by an *in vitro* kinase assay in which we incubated recombinant IRAK1 with regnase-1 and determined if IRAK1 modulated the interaction between regnase-1 and IKKβ (**Fig. 5c**). Coexpression of IRAK1 augmented the interaction between the regnase-1 and IKKβ (**Fig. 5d**).

Table 2 Change in regnase-1 mRNA half-life in response to IL-1β stimulation

Stimulation	20 min	240 min
Medium alone	49.2 ± 4.0	48.3 ± 5.3
IL-1β	132.1 ± 20.7	59.5 ± 6.7
TNF	60.1 ± 18.5	49.2 ± 11.6

Half-life of regnase-1 mRNA in HeLa cells before and 20 or 240 min after stimulation with IL-1β or TNF. Data are from three independent experiments (mean ± s.d.).

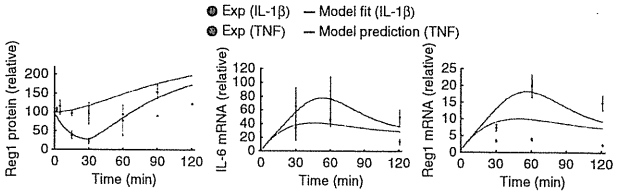

Figure 7 Computational modeling of the control of IL-6 mRNA expression by regnase-1. Expression of regnase-1 protein, IL-6 mRNA and regnase-1 mRNA in HeLa cells stimulated for 0–120 min (horizontal axes) with IL-1β (Exp (IL-1β)) or TNF (Exp (TNF)), followed by normalization to initial values (obtained from **Figs. 4b** and **6a**). Model fit (IL-1β), model values fit to the data after stimulation with IL-1β (fitted by COPASI 4.6 software for the simulation and analysis of biochemical networks and their dynamics[35]); Model prediction (TNF), corresponding model predictions for stimulation with TNF.

Furthermore, coexpression of IRAK1 resulted in considerable augmentation of the ubiquitination of regnase-1 induced by IKKβ (**Fig. 5e**). Collectively, these results suggested that IRAK1 facilitated regnase-1 ubiquitination mediated by IKKβ by direct interaction with and modification of regnase-1.

Regnase-1 protein controls regnase-1 mRNA

Once regnase-1 underwent rapid degradation in response to TLR or IL-1R stimuli, it reappeared within 60–120 min of stimulation. This required new synthesis of regnase-1 mRNA via transcription (**Supplementary Fig. 5**). Expression of regnase-1 mRNA in response to IL-1β is controlled by the transcription factors NF-κB and Elk-1 (ref. 28). Although NF-κB activation was induced similarly in HeLa cells in response to IL-1β or TNF (**Supplementary Fig. 11**), stimulation with IL-1β induced upregulation of regnase-1 mRNA, but stimulation with TNF did not (**Fig. 6a**). The half-life of regnase-1 mRNA was longer after 20 min of stimulation with IL-1β, but not after 20 min of stimulation with TNF (**Table 2**). In contrast, the half-life of regnase-1 mRNA was similar in unstimulated cells and those exposed to longer periods of stimulation with IL-1β (240 min; **Table 2**).

Those results prompted us to hypothesize that regnase-1 mRNA is a target of the regnase-1 RNase domain. To examine this possibility, we expressed constructs with β-globin-coding sequence and the 3′ UTR of regnase-1 or β-globin, plus the 'Tet-off' (tetracycline-regulated) gene-expression system (**Fig. 6b**). By halting new transcription with doxycycline, we were able to measure mRNA stability. Overexpression of regnase-1 resulted in rapid degradation of β-globin mRNA in the presence of the regnase-1 3′ UTR (**Fig. 6b,c**), which indicated that regnase-1 targeted regnase-1 mRNA via its 3′ UTR. Next we expressed luciferase reporter constructs with the entire 3′ UTR of regnase-1 (postions 1–865; numbered from the start of the 3′ UTR) in HEK293 cells (**Fig. 6d**). The luciferase activity decreased in response to coexpression of regnase-1 in a transfection dose-dependent manner (**Fig. 6e**). Furthermore, expression of a nuclease-inactive mutant of regnase-1 did not suppress the reporter activity (**Fig. 6e**), which indicated that regnase-1 controlled its own mRNA in a nuclease activity–dependent way. Next, by testing a set of luciferase constructs with truncation of the 3′ UTR of regnase-1, we found that positions 1–210 of the 3′ UTR produced regnase-1-mediated suppression, but positions 1–200 did not (**Supplementary Fig. 12**). We confirmed that the 3′ UTR (positions 192–210 of mouse regnase-1) was evolutionally conserved (**Supplementary Fig. 13**) and that the addition of this sequence to the β-globin 3′ UTR conferred responsiveness to regnase-1 overexpression (**Fig. 6e**). This sequence motif was predicted to form a stem-loop structure (**Fig. 6f**) like the regnase-1-responsive sequence in the 3′ UTR of IL-6 mRNA[22,29], and disruption of the stem-loop structure abrogated regnase-1-mediated suppression of the luciferase activity, whereas further insertion of mutations that restored the stem-loop structure 'rescued' the responsiveness of regnase-1 (**Fig. 6g**). These results suggested that the stem-loop structure present in the 3′ UTR of regnase-1 was required for regnase-1-mediated inhibition.

Mathematical modeling of the control of IL-6 mRNA

We next constructed a mathematical model that captured the activity of regnase-1 protein and regnase-1 and IL-6 mRNA based on biochemical equations with minimal assumptions (**Supplementary Fig. 14**). In the model, mRNA abundance was regulated via the digestion of mRNA by regnase-1 protein with experimentally determined degradation rates. The difference between stimulation with IL-1β and stimulation with TNF was described mathematically by constant degradation of regnase-1 protein for 30 min after stimulation with IL-1β, but not after stimulation with TNF. Whereas we determined the unknown parameters in the model by fitting only to the experimental data obtained after stimulation with IL-1β, the model qualitatively reproduced the kinetics after stimulation with TNF (**Fig. 7** and **Supplementary Table 2**). The differences in mRNA abundance after stimulation with IL-1β or TNF in this model resulted only from the digestion of mRNA by regnase-1 protein. These simulations indicated that our model captured the essence of the system dynamics.

DISCUSSION

Here we have shown that regnase-1 protein underwent dynamic modification in response to stimulation via TLRs or IL-1R. Regnase-1 was phosphorylated by the IKK complex, which led to its degradation by a ubiquitin-proteasome-dependent mechanism. Regnase-1 mutant proteins resistant to degradation showed more potency in suppressing IL-6 mRNA expression than did wild-type regnase-1. The expression of regnase-1 protein was induced in the later stage of TLR responses. Regnase-1 mRNA was controlled by regnase-1 protein via its 3′ UTR, which could contribute to reexpression of regnase-1 protein.

We found that expression of regnase-1 in resting cells prevented unwanted production of cytokines. The expression of IL-6 mRNA in unstimulated conditions was higher in regnase-1-deficient cells than in wild-type cells. This result suggested that transcriptional inhibition alone was not sufficient to shut down IL-6 mRNA completely. The trace amounts of proinflammatory cytokine–encoding mRNAs produced by background transcription should be degraded in resting cells by proteins such as regnase-1. Given that regnase-1-deficient mice spontaneously develop inflammatory disease, a dual locking system of inhibition of transcription and degradation of mRNA seems to be essential for the maintenance of homeostasis.

IKKs were identified as kinases responsible for the phosphorylation and degradation of IκBα, an inhibitor of NF-κB activation. The role of IKKs in the transcriptional activation of genes involved in inflammation has been studied extensively. In this study, we identified regnase-1 as a previously unsuspected substrate of IKK in response to activation via TLRs or IL-1R. It is notable that this single kinase complex regulated both gene transcription and mRNA stability in response to TLR stimulation. Although published studies have identified IKK substrates such as Bcl-10, SNAP23, p53 and IRF7 (refs. 30–33), only regnase-1 and IκBα were rapidly phosphorylated and degraded in response to activation of the IKK complex after stimulation via TLRs or IL-1β. A canonical DSGXXS motif is present in regnase-1 of various vertebrates, which suggests that the IKKβ-TrCP–mediated modification of regnase-1 is evolutionally conserved. Furthermore, rapid degradation

of regnase-1 allowed the cells to quickly express large amounts of cytokine mRNA in response to stimulation of TLRs or IL-1R.

We found that stimulation with IL-1β led to the degradation of regnase-1, but stimulation with TNF did not, although both cytokines activated the IKK complex. Furthermore, a MyD88-dependent signaling pathway was essential for extending the half-life of IL-6 mRNA, but a TRIF-dependent pathway was not, although both pathways led to IKK-mediated activation of NF-κB. We found that IRAK1 associated with and phosphorylated regnase-1. IRAK1 and IRAK2 were activated by IRAK4 and functioned redundantly in controlling the production of proinflammatory cytokines. It has been shown that IRAK1 as well as IRAK2 are critical for regulating the stability of cytokine-encoding mRNA, whereas TRAF6 is dispensable for IL-1α-induced stabilization of mRNA[26,27]. IRAK2 is reported to interact with the p38-activated kinase MK2, which inhibits the degradation of TNF mRNA by phosphorylating and sequestering tristetraprolin. Collectively, IRAKs may regulate mRNA stability by directly modulating various cellular proteins. However, further studies of the phosphorylation sites of regnase-1 are needed to identify the precise molecular mechanism by which IRAKs regulate mRNA stability in the TLR and IL-1R signaling pathway.

Notably, regnase-1 protein destabilized regnase-1 mRNA through its 3′ UTR. We identified an evolutionally conserved sequence element in regnase-1 transcript and found that this element can form a stem-loop structure. Disruption of the stem-loop structure abrogated regnase-1-mediated destabilization of mRNA. The regnase-1 target sequence found in IL-6 mRNA 3′ UTR is also reported to form a stem-loop structure. Thus, the stem-loop structure may be the target of regnase-1 for degradation, although further structural studies are required. IκBα mRNA is a target of NF-κB, and IKK-mediated degradation of IκBα leads to synthesis of IκBα protein, which suppresses inflammation. In this context, the self-feedback system can be a common mechanism for suppressing excess inflammation in the recovery phase of infection, as shown in our mathematical model.

A single domain in regnase-1 has dual RNase and deubiquitinase enzymatic functions, and regnase-1 negatively regulates Jnk and NF-κB signaling pathways[34]. In contrast, NF-κB activation in response to LPS is similar in wild-type and regnase-1-deficient macrophages[22], which indicates that regnase-1 is dispensable for the control of NF-κB signaling. We do not have an explanation for this discrepancy in the biological functions of regnase-1. As for the biochemical function of regnase-1, although it is theoretically possible for a single domain to function as both an RNase and a deubiquitinase, a survey of the Enzyme Commission codes for the numerical classification of enzymes among all entries in the UniProt Universal Protein Resource database showed that regnase-1 would be the first such domain of over 12 million entries. Moreover, we were unable to verify the reported homology between regnase-1 and the UCH deubiquitinase domain, for which there is a known structure[34]. On the basis of such preliminary investigations, we expect that further experiments will be needed to clarify the biochemical and biological roles of regnase-1.

The mathematical model qualitatively reproduced the kinetics of the system even after TNF stimulation. There were quantitative differences between the predicted and observed mRNA and protein abundance, however, especially for regnase-1 itself, which suggests that other factors are involved in its regulation. Nevertheless, it would be valuable for future studies of inflammation to translate experimental results into a theoretical framework.

Collectively, our study has demonstrated that IKK activity coupled rapid regulation of transcription and mRNA stability in the course of TLR responses. It is notable that regulators of gene transcription and mRNA stability were reciprocally controlled by a single kinase complex, and mRNA stability must be taken into account to understand the mechanisms of gene regulation in inflammation. These regulatory mechanisms can accomplish both suppression of unwanted inflammation and rapid production of proinflammatory cytokines in response to infection with pathogens.

METHODS

Methods and any associated references are available in the online version of the paper at http://www.nature.com/natureimmunology/.

Note: Supplementary information is available on the Nature Immunology website.

ACKNOWLEDGMENTS

We thank laboratory colleagues; E. Kamada and M. Kageyama for secretarial assistance; Y. Fujiwara, M. Kumagai and N. Umano for technical assistance; M. Takahama and T. Misawa for help with experiments; A. Matsuo, T. Hata, M. Tanaka and T. Kurimoto for discussions; K. Iwai (Osaka University) for expression plasmids for Flag-tagged β-TrCP and β-TrCPΔF; and D.V. Goeddel (Tularik; present affiliation, NGM Biopharmaceuticals) for the expression plasmid for IKKβ; I. Verma and M. Schmitt (Salk Institute), M. Schmidt-Supprian (Max Planck Institute) for MEFs deficient in IKKβ or both IKKα and IKKβ; S. Yamaoka (Tokyo Medical and Dental University) for Rat-1 and 5R cells; and F. Inagaki (Hokkaido University) for recombinant regnase-1 (amino acids 1–330). Supported by the Special Coordination Funds of the Japanese Ministry of Education, Culture, Sports, Science and Technology, and the Ministry of Health, Labour and Welfare in Japan, the Japan Society for the Promotion of Science through Funding Program for World-Leading Innovative R&D on Science and Technology (FIRST Program).

AUTHOR CONTRIBUTIONS

H.I. and O.T. designed and did most of the experiments and analyzed the data; K.M., T.U., K.K., T. Satoh and T. Saitoh helped with experiments; S.T. and D.M.S. did mathematical modeling; M.M. provided advice for experiments; H.I., S.T. and O.T. wrote the manuscript; and S.A. supervised the project.

COMPETING FINANCIAL INTERESTS

The authors declare no competing financial interests.

Published online at http://www.nature.com/natureimmunology/.
Reprints and permissions information is available online at http://www.nature.com/reprints/index.html .

1. Takeuchi, O. & Akira, S. Pattern recognition receptors and inflammation. *Cell* **140**, 805–820 (2010).
2. Beutler, B. Microbe sensing, positive feedback loops, and the pathogenesis of inflammatory diseases. *Immunol. Rev.* **227**, 248–263 (2009).
3. Medzhitov, R. & Horng, T. Transcriptional control of the inflammatory response. *Nat. Rev. Immunol.* **9**, 692–703 (2009).
4. Akira, S., Uematsu, S. & Takeuchi, O. Pathogen recognition and innate immunity. *Cell* **124**, 783–801 (2006).
5. Kawagoe, T. *et al.* Sequential control of Toll-like receptor-dependent responses by IRAK1 and IRAK2. *Nat. Immunol.* **9**, 684–691 (2008).
6. Skaug, B., Jiang, X. & Chen, Z.J. The role of ubiquitin in NF-κB regulatory pathways. *Annu. Rev. Biochem.* **78**, 769–796 (2009).
7. Xia, Z.P. *et al.* Direct activation of protein kinases by unanchored polyubiquitin chains. *Nature* **461**, 114–119 (2009).
8. Gerlach, B. *et al.* Linear ubiquitination prevents inflammation and regulates immune signalling. *Nature* **471**, 591–596 (2011).
9. Ikeda, F. *et al.* SHARPIN forms a linear ubiquitin ligase complex regulating NF-κB activity and apoptosis. *Nature* **471**, 637–641 (2011).
10. Tokunaga, F. *et al.* SHARPIN is a component of the NF-κB-activating linear ubiquitin chain assembly complex. *Nature* **471**, 633–636 (2011).
11. Karin, M. & Ben-Neriah, Y. Phosphorylation meets ubiquitination: the control of NF-κB activity. *Annu. Rev. Immunol.* **18**, 621–663 (2000).
12. Hayden, M.S. & Ghosh, S. Shared principles in NF-κB signaling. *Cell* **132**, 344–362 (2008).
13. Frescas, D. & Pagano, M. Deregulated proteolysis by the F-box proteins SKP2 and β-TrCP: tipping the scales of cancer. *Nat. Rev. Cancer* **8**, 438–449 (2008).
14. Baltimore, D. NF-kappaB is 25. *Nat. Immunol.* **12**, 683–685 (2011).
15. Oeckinghaus, A., Hayden, M.S. & Ghosh, S. Crosstalk in NF-κB signaling pathways. *Nat. Immunol.* **12**, 695–708 (2011).
16. Ea, C.K., Deng, L., Xia, Z.P., Pineda, G. & Chen, Z.J. Activation of IKK by TNFα requires site-specific ubiquitination of RIP1 and polyubiquitin binding by NEMO. *Mol. Cell* **22**, 245–257 (2006).

17. Karin, M. & Gallagher, E. TNFR signaling: ubiquitin-conjugated TRAFfic signals control stop-and-go for MAPK signaling complexes. *Immunol. Rev.* **228**, 225–240 (2009).
18. Anderson, P. Post-transcriptional control of cytokine production. *Nat. Immunol.* **9**, 353–359 (2008).
19. Hao, S. & Baltimore, D. The stability of mRNA influences the temporal order of the induction of genes encoding inflammatory molecules. *Nat. Immunol.* **10**, 281–288 (2009).
20. Anderson, P. Post-transcriptional regulons coordinate the initiation and resolution of inflammation. *Nat. Rev. Immunol.* **10**, 24–35 (2010).
21. Carballo, E., Lai, W.S. & Blackshear, P.J. Feedback inhibition of macrophage tumor necrosis factor-α production by tristetraprolin. *Science* **281**, 1001–1005 (1998).
22. Matsushita, K. *et al.* Zc3h12a is an RNase essential for controlling immune responses by regulating mRNA decay. *Nature* **458**, 1185–1190 (2009).
23. Yamamoto, M. *et al.* Role of adaptor TRIF in the MyD88-independent toll-like receptor signaling pathway. *Science* **301**, 640–643 (2003).
24. Yamaoka, S. *et al.* Complementation cloning of NEMO, a component of the IκB kinase complex essential for NF-κB activation. *Cell* **93**, 1231–1240 (1998).
25. Spencer, E., Jiang, J. & Chen, Z.J. Signal-induced ubiquitination of IκBα by the F-box protein Slimb/β-TrCP. *Genes Dev.* **13**, 284–294 (1999).
26. Hartupee, J., Li, X. & Hamilton, T. Interleukin 1α-induced NFκB activation and chemokine mRNA stabilization diverge at IRAK1. *J. Biol. Chem.* **283**, 15689–15693 (2008).
27. Wan, Y. *et al.* Interleukin-1 receptor-associated kinase 2 is critical for lipopolysaccharide-mediated post-transcriptional control. *J. Biol. Chem.* **284**, 10367–10375 (2009).
28. Kasza, A. *et al.* Transcription factors Elk-1 and SRF are engaged in IL1-dependent regulation of ZC3H12A expression. *BMC Mol. Biol.* **11**, 14 (2010).
29. Paschoud, S. *et al.* Destabilization of interleukin-6 mRNA requires a putative RNA stem-loop structure, an AU-rich element, and the RNA-binding protein AUF1. *Mol. Cell. Biol.* **26**, 8228–8241 (2006).
30. Wu, C.J. & Ashwell, J.D. NEMO recognition of ubiquitinated Bcl10 is required for T cell receptor-mediated NF-κB activation. *Proc. Natl. Acad. Sci. USA* **105**, 3023–3028 (2008).
31. Suzuki, K. & Verma, I.M. Phosphorylation of SNAP-23 by IκB kinase 2 regulates mast cell degranulation. *Cell* **134**, 485–495 (2008).
32. Xia, Y. *et al.* Phosphorylation of p53 by IκB kinase 2 promotes its degradation by β-TrCP. *Proc. Natl. Acad. Sci. USA* **106**, 2629–2634 (2009).
33. Hoshino, K. *et al.* IκB kinase-α is critical for interferon-α production induced by Toll-like receptors 7 and 9. *Nature* **440**, 949–953 (2006).
34. Liang, J. *et al.* MCP-induced protein 1 deubiquitinates TRAF proteins and negatively regulates JNK and NF-κB signaling. *J. Exp. Med.* **207**, 2959–2973 (2010).
35. Hoops, S. *et al.* COPASI—a COmplex PAthway SImulator. *Bioinformatics* **22**, 3067–3074 (2006).

The TRAF-associated protein TANK facilitates cross-talk within the IκB kinase family during Toll-like receptor signaling

Kristopher Clark[a], Osamu Takeuchi[b], Shizuo Akira[b], and Philip Cohen[a,1]

[a]Medical Research Council Protein Phosphorylation Unit, College of Life Sciences, Sir James Black Centre, University of Dundee, Dundee, DD1 5EH, Scotland, United Kingdom; and [b]Laboratory of Host Defense, World Premier International Immunology Frontier Research Center, Osaka University, Osaka 565-0871, Japan

Contributed by Philip Cohen, August 30, 2011 (sent for review May 20, 2011)

Toll-like receptor (TLR) ligands that signal via TIR-domain-containing adapter-inducing IFNβ (TRIF) activate the IκB kinase (IKK)-related kinases, TRAF associated NFκB activator (TANK)-binding kinase-1 (TBK1) and IKKε, which then phosphorylate IRF3 and induce the production of IFNβ. Here we show that TBK1 and IKKε are also activated by TLR ligands that signal via MyD88. Notably, the activation of IKKε is rapid, transient, and it precedes a more prolonged activation of TBK1. The MyD88- and TRIF-dependent signaling pathways activate the IKK-related kinases by two signaling pathways. One is mediated by the canonical IKKs, whereas the other culminates in the autoactivation of the IKK-related kinases. Once activated, TBK1/IKKε then phosphorylate and inhibit the canonical IKKs. The negative regulation of the canonical IKKs by the IKK-related kinases occurs in both the TRIF- and MyD88-dependent TLR pathways, whereas IRF3 phosphorylation is restricted to the TRIF-dependent signaling pathway. We have discovered that the activation of IKKε is abolished, the activation of TBK1 is reduced, and the interaction between the IKK-related kinases and the canonical IKKs is suppressed in TANK$^{-/-}$ macrophages, preventing the IKK-related kinases from negatively regulating the canonical IKKs. In contrast, IRF3 phosphorylation and IFNβ production was normal in TANK$^{-/-}$ macrophages. Our results demonstrate a key role for TANK in enabling the canonical IKKs and the IKK-related kinases to regulate each other, which is required to limit the strength of TLR signaling and ultimately, prevent autoimmunity.

Toll-like receptors (TLRs) respond to components of pathogens leading to the activation of several signaling pathways that culminate in the production of inflammatory mediators to combat the invading pathogen. However, there is mounting evidence that disregulation of TLR signaling pathways can lead to the overproduction of inflammatory mediators resulting in the development of inflammatory and autoimmune diseases (e.g., refs. 1, 2). Understanding the mechanisms that prevent the excessive production of inflammatory mediators may identify novel drug targets for treating these diseases.

TLRs initiate signal transduction pathways using two receptor-proximal protein adaptors, called MyD88 and TIR-domain-containing adapter-inducing IFNβ (TRIF) (3). TLRs 1, 2, and 5–9 signal via MyD88; TLR3 signals via TRIF; and TLR4 signals via both MyD88 and TRIF (3). In the MyD88-dependent pathway, an E3 ubiquitin ligase TRAF6, generates K63-linked polyubiquitin (K63-pUb) chains, which activate the protein kinase TAK1 (4, 5). These K63-pUb chains also interact with NFκB essential modulator (NEMO), a component of the canonical IKK complex (6, 7), inducing a conformational change that facilitates the activation of this complex by TAK1 and by autophosphorylation (8, 9). Subsequently, the canonical IKKs (IKKα and IKKβ) activate downstream targets, which include the protein kinase Tpl2 (10, 11) and the transcription factor NFκB (12) stimulating the production and secretion of inflammatory mediators, such as TNFα, IL-6, and IL-12. Engagement of the TRIF-dependent pathway also leads to the activation of two other members of the IKK subfamily of protein kinases, TRAF associated NFκB activator (TANK)-binding kinase-1 (TBK1) and IKKε, termed the IKK-related kinases (3, 12). TBK1/IKKε then phosphorylate the transcription factor IRF3, leading to its dimerization and nuclear translocation where it stimulates the transcription of genes, such as IFNβ, to set up an antiviral state (13–16). For these reasons, the IKK-related kinases have been thought to play separate roles from the canonical IKKs during innate immunity.

Recently, we found that in pathways triggered by TLR3 and TLR4 in macrophages, the IKK-related kinases and the canonical IKKs are interconnected in a signaling network required to balance their respective catalytic activities (9). The activation of the IKK-related protein kinases requires their phosphorylation at Ser172 and occurs by two distinct signaling pathways. One involves the direct phosphorylation of TBK1 and IKKε by the canonical IKKs, whereas the second culminates in the autoactivation of the IKK-related kinases (9). Once activated, the IKK-related kinases phosphorylate the catalytic and regulatory subunits of the canonical IKK complex on sites that inhibit their catalytic activity (9). This network prevents the hyperactivation of the IKK-family members and raises the question of how they interact with one another to control innate immunity.

The regulatory proteins that control the activation of the IKK-related kinases have yet to be fully defined. TBK1 and IKKε interact via their C termini with TANK, NFκB activating kinase (NAK)-associated protein 1 (NAP1) and similar to NAP1 TBK1 adaptor (Sintbad) (17–19), but only TBK1 interacts with optineurin (20). It has therefore been suggested that distinct forms of the IKK-related kinases may be present in cells, each comprising a catalytic subunit and a different regulatory subunit, which are involved in regulating different aspects of innate immunity (21). The recent characterization of the TANK$^{-/-}$ mouse led to the unexpected finding that TANK is not required for the production of IFNβ in response to viral infection, but instead is required to limit MyD88-dependent TLR signaling and so prevent the development of autoimmune nephritis (1). How TANK negatively regulates TLR signaling remains poorly defined. Notably, macrophages from the TANK$^{-/-}$ mice displayed increased NFκB signaling in response to TLR ligands (1). Because TANK, but not the TBK1 and IKKε catalytic subunits, is reported to interact with NEMO (22, 23), we reasoned that TANK may represent a key component of a molecular bridge that facilitates the "cross-talk" between the IKK-related kinases and the canonical IKKs. In this

Author contributions: K.C. and P.C. designed research; K.C. performed research; O.T. and S.A. contributed new reagents/analytic tools; K.C. and P.C. analyzed data; and K.C. and P.C. wrote the paper.

The authors declare no conflict of interest.

Freely available online through the PNAS open access option.

[1]To whom correspondence should be addressed. E-mail: p.cohen@dundee.ac.uk.

This article contains supporting information online at www.pnas.org/lookup/suppl/doi:10.1073/pnas.1114194108/-/DCSupplemental.

paper, we have therefore investigated this hypothesis by studying the activation of, and cross-talk between, the IKK family members in TANK$^{-/-}$ macrophages in response to MyD88- and TRIF-dependent agonists.

Results

Activation of TBK1 and IKKε by MyD88- and TRIF-Dependent TLR Agonists. Recently, we discovered that TBK1 and IKKε are activated by the MyD88-dependent cytokine IL-1α in fibroblasts, which signals exclusively via MyD88 (24). We therefore investigated whether the IKK-related kinases were also activated in bone marrow-derived macrophages (BMDMs) by MyD88-dependent TLR agonists (Fig. 1 *A–D* and Fig. S1). Ligands that signal via MyD88, namely Pam_3CSK_4 (TLR1/2), lipoteichoic acid (LTA; TLR2/6), R837 (TLR7), and CpG (TLR9) activated TBK1 and IKKε at least as robustly as the synthetic dsRNA mimetic poly(I:C) (TLR3), which signals via TRIF, or LPS (TLR4), which signals via TRIF and MyD88. However, the kinetics of activation differed between agonists and between the IKK-related kinases themselves. In general, the peak of IKKε activity preceded that of TBK1, a rapid and transient activation of IKKε being followed by a slower and more sustained activation of TBK1. Importantly, LTA, Pam_3CSK_4, poly(I:C), R837 and CpG induced the activation of TBK1 and IKKε in BMDMs from the LPS-insensitive mouse strain C3H/HeJ, demonstrating that the ability of the different MyD88-dependent TLR agonists to activate the IKK-related kinases was not due to contamination with endotoxin (Fig. 1*E*).

IKKε is also called "IKK-inducible" (IKKi), because its expression is enhanced by prolonged exposure to proinflammatory stimuli (25) through an NFκB-dependent pathway driven by the canonical IKKs (9). We showed that the LPS-stimulated activation of IKKε peaks at 10 min and then decreases to a low level by 60 min, which is sustained for the next 24 h, even though LPS (Fig. S2*A*) and other TLR agonists (Fig. S2*B*) greatly increase IKKε protein expression over this period. Thus, a high level of IKKε protein expression does not correlate with high IKKε activity in mouse macrophages.

We next studied the activation of the IKK-related kinases in MyD88$^{-/-}$ and TRIF$^{-/-}$ macrophages. As expected, the activation of TBK1 and IKKε by Pam_3CSK_4, R837, and CpG was abolished in MyD88$^{-/-}$ macrophages but was normal in TRIF$^{-/-}$ macrophages (Fig. S3 *A*, *C*, and *D*), whereas the poly(I:C)-mediated activation of TBK1 and IKKε was normal in MyD88$^{-/-}$ macrophages but absent in TRIF$^{-/-}$ macrophages (Fig. S3*B*). However, of particular note was the finding that LPS was able to induce the activation of TBK1 and IKKε via the MyD88-dependent and the TRIF-dependent pathway, although with different kinetics. In MyD88$^{-/-}$ BMDMs, the LPS-induced activation of the IKK-related kinases was reduced, delayed until 30 min, and transient, returning to near basal levels after 1–2 h

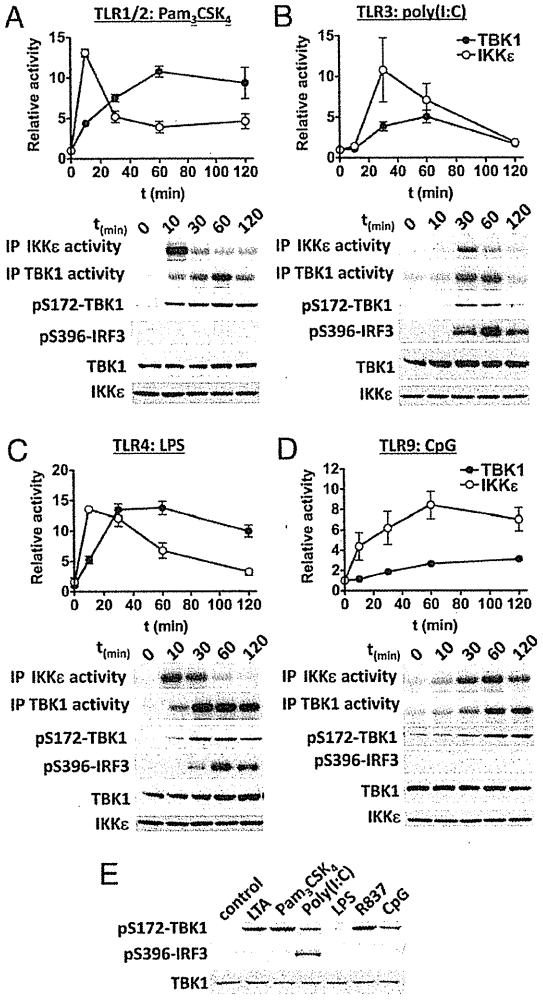

Fig. 1. Kinetics of activation of TBK1 and IKKε by different TLR agonists. BMDMs were stimulated for the times indicated with (*A*) 1 μg/mL Pam_3CSK_4, (*B*) 10 μg/mL poly(I:C), (*C*) 100 ng/mL LPS, or (*D*) 2 μM CpG. TBK1 and IKKε were immunoprecipitated (IP) and their catalytic activities were measured by incubating the immunoprecipitated kinases with GST-IRF3 and Mg[γ-^{32}P]-ATP. Reactions were terminated in SDS, the proteins resolved by SDS/PAGE, and the gel autoradiographed (*A–D*, *Upper* two panels). Kinase activity was quantified by phosphorimager analysis (mean ± SEM, n = 3–6). An aliquot of each immunoprecipitation was also immunoblotted for TBK1 and IKKε as a loading control (*Lower*). Cell extract (20 μg protein) was additionally immunoblotted with antibodies that recognize TBK1 phosphorylated at Ser172 (to monitor activation by a second independent method) and for the phosphorylation of IRF3 at Ser396 (*A–D*, *Lower* three panels). (*E*) BMDMs from the LPS-resistant mouse strain C3H/HeJ were stimulated for 60 min with 2 μg/mL LTA, 1 μg/mL Pam_3CSK_4, 10 μg/mL poly(I:C), 100 ng/mL LPS, 2 μg/mL R837 or 2 μM CpG. Cell extracts (20 μg protein) were immunoblotted with the same antibodies used in *A–D*.

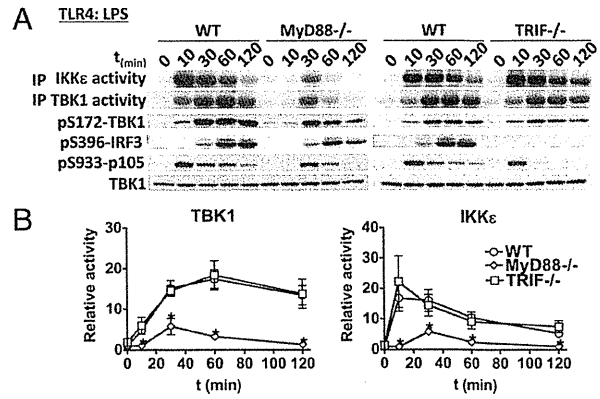

Fig. 2. Activation of TBK1 and IKKε in response to LPS occurs via both the MyD88- and the TRIF-dependent pathways, but only the latter leads to the phosphorylation of IRF3. (*A*) BMDMs from MyD88$^{-/-}$ or TRIF$^{-/-}$ mice or WT littermates were stimulated for the times indicated with 100 ng/mL LPS. The catalytic activities of TBK1 and IKKε (*A*, *Upper* two panels) were measured as described in Fig. 1 and *Materials and Methods*. Cell extracts (20 μg protein) were immunoblotted with the antibodies indicated (*A*, *Lower* four panels). (*B*) Quantitation of TBK1 and IKKε activities by phosphorimager analysis (mean ± SEM, n = 3).

(Fig. 2), whereas in TRIF$^{-/-}$ macrophages, the activation of TBK1 and IKKε by LPS was similar to wild-type (WT) macrophages (Fig. 2). Thus, the IKK-related kinases are activated by both the MyD88- and TRIF-dependent signaling pathways in macrophages. The LPS-stimulated activation of the canonical IKKs (monitored by the phosphorylation of p105, an established substrate of IKKβ (26)) paralleled that of IKKε, becoming maximal after 10 min in TRIF$^{-/-}$ BMDMs and after 30 min in MyD88$^{-/-}$ BMDMs (Fig. 2).

Phosphorylation of IRF3 by the IKK-Related Kinases Occurs Only via the TRIF-Dependent Signaling Pathway. It is well established that the IKK-related kinases phosphorylate IRF3 in a TRIF-dependent pathway that is activated by TLR3 and TLR4 ligands (in the Introduction) and a strict correlation between the induction of IRF3 phosphorylation at Ser396 and coupling to TRIF was observed in the present study (Fig. 1 *B*, *C*, and *E* and Fig. 2). Poly(I:C) and LPS stimulated the phosphorylation of IRF3 (Fig. 1 *B* and *C*), but all of the MyD88-dependent TLR agonists tested failed to induce any phosphorylation of IRF3 (Fig. 1*E*), although they activated TBK1 and IKKε at least as robustly (Fig. 1). Moreover, the LPS-stimulated phosphorylation of IRF3 was not impaired in MyD88-deficient macrophages (Fig. 2*A*), even though far lower TBK1/IKKε activity was generated in these cells. Furthermore, LPS failed to induce IRF3 phosphorylation in TRIF-deficient macrophages, even though the activation of the IKK-related kinases was similar to WT macrophages (Fig. 2*B*).

Cross-Talk Between the Canonical IKKs and IKK-Related Kinases During MyD88-Dependent Signaling in Macrophages. We have shown previously that the activation of the IKK-related kinases by IL-1α in fibroblasts or LPS and poly(I:C) in RAW264.7 cells requires two signaling pathways. One of these is IKKα/β dependent, whereas the other appears to culminate in the autoactivation of the IKK-related kinases, because it can be prevented by pharmacological inhibition of TBK1/IKKε (9). In the present study, we found that Pam_3CSK_4, a MyD88-dependent agonist, also activated TBK1 and IKKε by these two pathways in primary BMDMs (Fig. 3*A*). Thus, incubation of BMDMs with the TAK1 inhibitor 5Z-7-oxozeaenol, which prevents the activation of IKKβ and the phosphorylation of its substrate p105 (Fig. 3*B*), partially suppressed the Pam_3CSK_4-stimulated activation of TBK1 and IKKε (Fig. 3*A*). In contrast, incubation with the TBK1/IKKε inhibitor MRT67307 (9) increased the activation of these IKK-related kinases, but incubation with both inhibitors abolished activation (Fig. 3*A*). The enhanced activation of TBK1 and IKKε when cells are incubated with MRT67307, and which is abolished by inhibition of TAK1 (Fig. 3*A*), has been noted previously in IL-1–stimulated fibroblasts and LPS-stimulated RAW264.7 cells (24), and indicates that TBK1/IKKε control a negative feedback loop that suppresses their activation by the canonical IKKs.

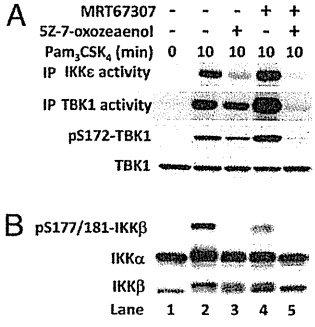

Fig. 3. Cross-talk between the canonical IKKs and the IKK-related kinases during MyD88 signaling in macrophages. (*A*) Activation of the IKK-related kinases. BMDMs were treated for 1 h with either 1 μM 5Z-7-oxozeaenol, 2 μM MRT67307, or both kinase inhibitors before stimulation for 10 min with 1 μg/mL Pam_3CSK_4. The catalytic activities of TBK1 and IKKε (*Upper* two panels) were measured as in Fig. 1 and *Materials and Methods*. In these experiments, TBK1 and IKKε were immunoprecipitated from the cell extracts and the immunoprecipitates washed to remove MRT67307 before assaying in the absence of this compound, because MRT67307 is a reversible inhibitor of the IKK-related kinases. Cell extracts (20 μg protein) were also immunoblotted with the antibodies indicated (*Lower* two panels). (*B*) The cell extracts in *A* were immunoblotted with the antibodies indicated. The phospho-specific antibody that recognizes IKKβ phosphorylated at Ser177 and Ser181 also recognizes IKKα phosphorylated at Ser176 and Ser180. However, the bands shown correspond to phosphorylated IKKβ only. Phosphorylated IKKα migrates more rapidly than IKKβ and is recognized very poorly by the antibody (figure S1A in ref. 9), which may be explained by lower levels of expression and/or activation of IKKα compared with IKKβ.

The TAK1-dependent activation of the canonical IKKs can be monitored by the phosphorylation of two serine residues in their activation loops (Ser177 and Ser181 of IKKβ). Once activated, the canonical IKKs are subsequently inhibited by the phosphorylation of amino acid residues distinct from those located in the activation loops, and which are targeted by the canonical IKKs themselves (27) and by the IKK-related kinases (9). The phosphorylation of these inhibitory sites can be monitored by a retardation in the electrophoretic mobility of IKKα and IKKβ, which is reversed by phosphatase treatment (9). In the present study, we found that Pam_3CSK_4 induced a decrease in the electrophoretic mobility of IKKα and IKKβ (Fig. 3*B*, lane 2), which was partially suppressed by inhibition of TAK1 (Fig. 3*B*, compare lanes 2 and 3) or the IKK-related kinases (Fig. 3*B*, compare lanes 2 and 4), and prevented by the combined inhibition of all four IKKs (Fig. 3*B*, compare lanes 2 and 5). Pharmacological inhibition of the IKK-related kinases increased the activity of IKKα and IKKβ as shown by the increased phosphorylation of TBK1 and IKKε, which was blocked by inhibition of TAK1 (Fig. 3*A*). Thus, the cross-talk between the different members of the IKK family is conserved among the different TLR signaling pathways in macrophages.

To verify that MRT67307 exerts its effect by inhibition of the IKK-related kinases, and not by an off-target effect, we carried out further experiments with mouse embryonic fibroblasts (MEFs) from mice that do not express TBK1 and IKKε. The IL-1α stimulated phosphorylation of the IKKβ substrates p105 (26) and RelA (9) was enhanced in MEFs that do not express the IKK-related kinases (Fig. S4*A*). Moreover, the IL-1–induced retardation in the electrophoretic mobility of IKKβ was much less pronounced in MEFs lacking the IKK-related kinases (Fig. S4*B*). It should be noted that the more striking enhancement in the phosphorylation of p105 seen in IL-1α–stimulated TBK1/IKKε double knockout (DKO) MEFs in Fig. S4*A* is explained by the use of 10-fold lower concentrations of IL-1α than those used in Fig. S4*B*.

Cross-Talk Within the IKK Family Requires the Adaptor Protein TANK. The finding that the IKK-related kinases are activated by the MyD88-dependent signaling pathway raised the question of which binding partners of TBK1 and IKKε might be important for their activation via this pathway. Because TBK1 was originally discovered as a protein that interacts with TANK (17), we studied the catalytic activity of TBK1 and IKKε in BMDMs from WT and TANK$^{-/-}$ mice in response to Pam_3CSK_4, LPS, and CpG (Fig. 4). Strikingly, the catalytic activity of IKKε was not stimulated by any TLR agonist tested in the TANK$^{-/-}$ macrophages. The phosphorylation and activation of TBK1 was also reduced at the earliest time points examined, but not abolished (Fig. 4). These results demonstrate that TANK is absolutely required for the activation of IKKε activation by TLR ligands but not for the activation of TBK1 in mouse macrophages. In contrast, the LPS-stimulated phosphorylation of IRF3 and pro-

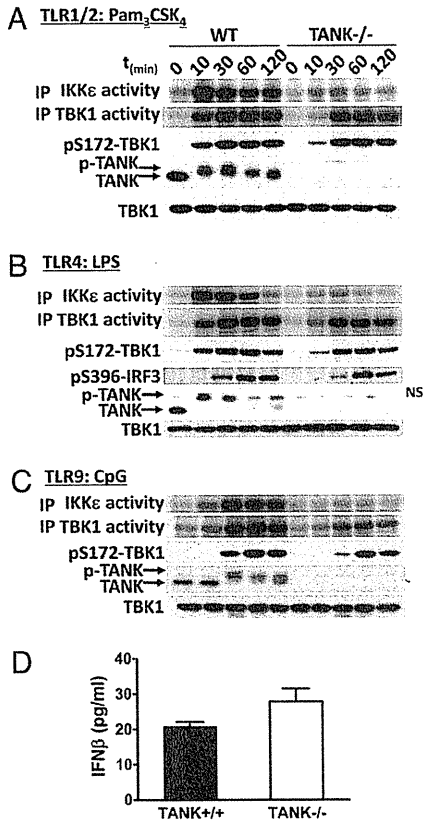

Fig. 4. TANK is required for efficient activation of the IKK-related kinases by TLR agonists. (*A–C*) BMDMs from TANK$^{-/-}$ mice or WT littermates were stimulated for the times indicated with (*A*) 1 μg/mL Pam_3CSK_4, (*B*) 100 ng/mL LPS, or (*C*) 2 μM CpG. The catalytic activities of TBK1 and IKKε (*A–C*, *Upper* two panels) were measured as described in Fig. 1 and *Materials and Methods*. Cell extracts (20 μg protein) were also immunoblotted with the antibodies indicated (*A* and *C*, *Lower* three panels and *B*, *Lower* four panels). NS in *B* denotes a nonspecific band detected by the TANK antibody. (*D*) BMDMs from TANK$^{-/-}$ mice or WT littermates were stimulated for 6 h with 100 ng/mL LPS and the concentration of IFNβ in the culture supernatant measured with the ELISA kit from R&D Systems (mean ± SEM, $n = 3$).

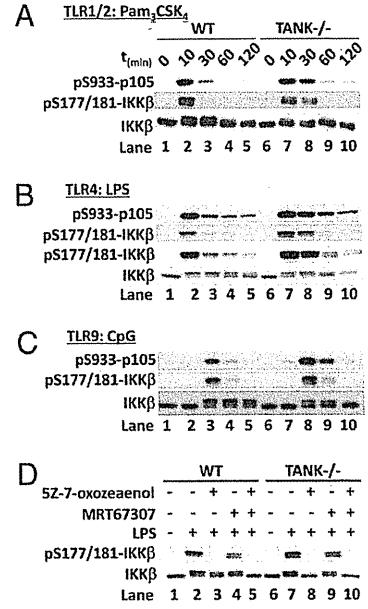

Fig. 5. Negative regulation of the canonical IKKs by the IKK-related kinases is impaired in TANK$^{-/-}$ macrophages. BMDMs from TANK$^{-/-}$ mice or WT littermates were stimulated for the times indicated with (*A*) 1 μg/mL Pam_3CSK_4, (*B*) 100 ng/mL LPS, or (*C*) 2 μM CpG. Cell extracts (20 μg protein) were immunoblotted with the antibodies indicated. (*D*) BMDMs from TANK$^{-/-}$ mice or WT (TANK$^{+/+}$) littermates were treated for 1 h with 1 μM 5Z-7-oxozeaenol, and/or 2 μM MRT67307, before stimulation for 10 min with 100 ng/mL LPS. Cell extracts were immunoblotted as described above.

duction of IFNβ was similar in BMDMs from TANK$^{-/-}$ and WT mice (Fig. 4 *B* and *D*). This is consistent with our previous observation that TANK was not required for IFNα production in dendritic cells after infection by Newcastle disease virus (1).

The TLR ligands also induced a striking decrease in the electrophoretic mobility of TANK, which is caused by phosphorylation (28). The phosphorylation of TANK was partially suppressed by pharmacological inhibition of the IKK-related kinases, partially suppressed by inhibition of the canonical IKKs, and completely prevented by inhibition of all of the IKK family members (9). Thus, TANK is phosphorylated by all of the IKK family members, but the role of phosphorylation has yet to be elucidated.

We next investigated how the absence of TANK affected the activity of IKKβ. Stimulation of TANK$^{-/-}$ BMDMs with TLR ligands led to a more prolonged and/or enhanced activation of IKKβ, as judged by the phosphorylation of the serine residues positioned in the activation loop and by the phosphorylation of its substrate p105 (Fig. 5 *A–C*), suggesting that TANK is required for the negative regulation of the canonical IKKs. There was also a smaller reduction in the electrophoretic mobility (phosphorylation) of IKKβ in the TANK$^{-/-}$ macrophages than in the WT macrophages (Fig. 5 *A* and *B*, compare lanes 2 and 7 or Fig. 5*C*, compare lanes 3–5 and 8–10). Because the activation of IKKε was abolished and the activation of TBK1 was reduced in the TANK$^{-/-}$ macrophages (Fig. 4), the simplest explanation for these results is that the activity of the IKK-related kinases is insufficient to mediate the negative regulation of the canonical IKKs in these cells.

If the negative regulation of IKKβ by the IKK-related kinases is lost in BMDMs from TANK$^{-/-}$ mice, then the decrease in the electrophoretic mobility of IKKβ induced by TLR ligands should result solely from phosphorylation by TAK1 and subsequent autophosphorylation by IKKβ and therefore be prevented by the inhibition of TAK1 alone. This prediction was verified by the finding that the TAK1 inhibitor 5Z-7-oxozeaenol blocked the LPS-stimulated decrease in the mobility of IKKβ in TANK$^{-/-}$ macrophages (Fig. 5*D*, *Lower*, lanes 6–8), but the combination of 5Z-7-oxozeaenol and the TBK1/IKKε inhibitor MRT67307 was required to obtain a similar effect in WT macrophages (Fig. 5*D*, lanes 1–5). These studies establish that TANK is required for the activation of IKKε and contributes to the activation of TBK1, and that the cross-talk between the canonical IKKs and the IKK-related kinases during TLR signaling is disrupted in TANK$^{-/-}$ macrophages.

TANK Is Required for the Interaction of the IKK-Related Kinases with the Canonical IKK Complex. TANK has been reported to bind to NEMO (23), suggesting that TANK might be important for interaction between the IKK-related kinases and the canonical IKKs to facilitate cross-talk between the different IKK family members. We therefore initially investigated whether an interaction between the canonical IKKs and the IKK-related kinases could be detected in macrophages. We immunoprecipitated TBK1 from the cell extracts and immunoblotted for the presence of components of the canonical IKK complex or, conversely, immunoprecipitated NEMO or IKKβ and immuno-

blotted for the presence of components of the IKK-related kinases. These experiments showed that IKKα, IKKβ, and NEMO could be immunoprecipitated with anti-TBK1, whereas TANK, TBK1, and IKKε could be immunoprecipitated with either anti-NEMO or anti-IKKβ, but not by control IgG (Fig. 6*A*). Strikingly, the IKKβ antibody was unable to immunoprecipitate IKKε from extracts of TANK$^{-/-}$ macrophages, whereas the amount of TBK1 that could be immunoprecipitated was reduced considerably. In contrast, the ability of anti-IKKβ to immunoprecipitate IKKα and NEMO was unaffected (Fig. 6*B*). These experiments demonstrate that the IKK-related kinases and the canonical IKKs interact in macrophages and that the presence of TANK is critical for the formation of these complexes.

Discussion

In this paper we show that TANK is required for the activation of IKKε, that it contributes to the early phase of activation of TBK1, and that it is required for the interaction of the IKK-related kinases with the canonical IKKs. These findings can explain why the negative regulation of the canonical IKKs by the IKK-related kinases is lost in TANK$^{-/-}$ macrophages leading to enhanced activation of the canonical IKKs. Thus, an important role for TANK is to facilitate the activation of the IKK-related kinases and couple them to the canonical IKKs allowing for efficient cross-talk between them during TLR signaling. We also establish that, similar to the IL-1–stimulated MyD88-dependent pathway that we described recently in MEFs (9), the activation of the IKK-related kinases by TLR ligands occurs via two pathways in BMDMs, one mediated by the canonical IKKs and the other by a pathway that culminates in the autoactivation of the IKK-related kinases (9). On the basis of these findings and other information in the literature, we propose the following model for the regulation of the IKK family of protein kinases (Fig. 7). When TLR signaling pathways are activated by the MyD88-dependent pathway, K63-pUb chains generated by the action of TRAF6 bind to the TAB2 and TAB3 regulatory components of the TAK1 complex, inducing conformational changes that trigger the autoactivation of TAK1 (8). The K63-pUb chains also interact with NEMO, a component of the canonical IKK complex. This induces conformational changes that allow TAK1 to initiate activation of the canonical IKK complex (29). Because the canonical IKK complex interacts with the IKK-related kinases (Fig. 6*A*) via TANK (Fig. 6*B*), which has itself been reported to interact with NEMO (23), the binding

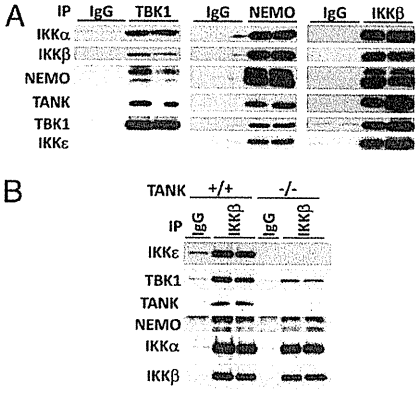

Fig. 6. Association of the canonical IKKs and IKK-related kinases is dependent on TANK. (*A*) Lysates of RAW264.7 macrophages were incubated with antibodies from nonimmunized sheep (IgG) or antibodies against TBK1, NEMO, or IKKβ. The immunoprecipitates were washed, separated by SDS/PAGE, and immunoblotted with the antibodies indicated. (*B*) Cell extracts from TANK$^{+/+}$ and TANK$^{-/-}$ macrophages were used to immunoprecipitate IKKβ and coimmunoprecipitating proteins were monitored by immunoblotting.

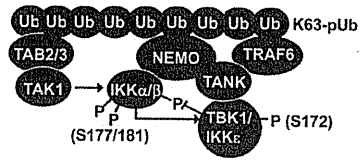

Fig. 7. Model for the cross-talk between IKK family members in the MyD88 signaling pathway. K63-pUb chains formed by TRAF6 in response to IL-1 or TLR stimulation bind to TAB2/3–TAK1 and IKKα/β–NEMO–TANK–TBK1/IKKε complexes enabling the sequential activation of the canonical IKKs by TAK1 and then the activation of the IKK-related kinases by the canonical IKKs and by autoactivation, as discussed in the text. The IKK-related kinases then negatively regulate the canonical IKKs by phosphorylating sites that inhibit activity.

of K63-pUb chains to NEMO may induce conformational changes in the TANK–IKKε and TANK–TBK1 complexes that allow them to be activated by the canonical IKKs and by autophosphorylation. This proposal can explain why NEMO is required for both the activation of the IKK-related kinases by the pathway that is independent of the canonical IKKs and for direct activation by the canonical IKKs (9). The TANK-dependent interaction between the IKK-related kinases and the canonical IKK complex also permits the IKK-related kinases to phosphorylate inhibitory sites on IKKα/β and so dampen their catalytic activity and the production of inflammatory mediators (Fig. 7). The IKK-related kinases and the canonical IKKs additionally phosphorylate NEMO and TANK (9), but the contribution that these phosphorylation events make to cross-talk between the different members of the IKK subfamily has yet to be determined.

One of our laboratories has reported that macrophages from TANK$^{-/-}$ mice show increased TRAF6 polyubiquitylation in response to TLR7 stimulation, implying that the E3 ligase activity of TRAF6 is enhanced (1). Interestingly, TANK was originally identified as a protein that interacts with different members of the TRAF family (30, 31) and TANK may be able to bind simultaneously to NEMO and TRAF6 because these two proteins bind to distinct regions of TANK (23, 30). An intriguing possibility is that the interaction of TRAF6 with TANK may enable the IKK-related kinases to phosphorylate and negatively regulate TRAF6, explaining why TRAF6 E3 ligase activity is enhanced on TANK$^{-/-}$ macrophages. Alternatively, or in addition, the IKK-related kinases may negatively regulate one or more "upstream" components of the signaling pathway that leads to the activation of TRAF6. Thus, the IKK-related kinases may negatively regulate TLR–MyD88 signaling pathway in several ways. This may explain why TANK$^{-/-}$ mice overproduce IL-6 and other inflammatory mediators and develop autoimmune nephritis, which can be prevented by crossing to MyD88-deficient mice (1). It would therefore be more appropriate if the acronym TANK stood for "TRAF-associated NFκB inhibitor" and not "TRAF-associated NFκB activator."

We also found that TANK was dispensable for IRF3 phosphorylation and IFNβ production in response to LPS (Fig. 4 *B* and *D*), even though the LPS-stimulated activation of IKKε was abolished. Similarly, LPS-stimulated TBK1 activity was greatly decreased in MyD88$^{-/-}$ macrophages without affecting the phosphorylation of IRF3 (Fig. 2). These observations suggest that a form of TBK1, distinct from the TBK1–TANK complex, and which accounts for only a minor proportion of the total TBK1 activity that we measure in BMDM extracts, mediates the phosphorylation of IRF3 in vivo.

A further unresolved question is why TLR agonists that signal via MyD88 activate the IKK-related kinases robustly without inducing any phosphorylation of IRF3 (Fig. 1 and Fig. S1), even though the activated IKK-related kinases can phosphorylate IRF3 in vitro. These findings indicate that, although the IKK-related kinases are required for the phosphorylation of IRF3

in vivo, their activation is not sufficient and an additional molecular determinant(s) is (are) required to couple TBK1 to the phosphorylation of IRF3. One determinant could be the formation of a TLR3/4–TRIF–TRAF3 complex at the endosomal membrane (32), because the phosphorylation of IRF3 and production of IFNβ by this pathway does not occur in TRAF3$^{-/-}$ macrophages (33, 34). The requirement to colocalize a TLR with TRAF3 at a membrane to produce IFNβ has been elegantly demonstrated by targeting TRAF3 to the plasma membranes of macrophages, which permitted TLR2 agonists that signal via MyD88 to induce high levels of IFNβ, which does not happen if TRAF3 is not targeted to these membranes (32). For these reasons, TRAF3 has been widely believed to operate upstream of the IKK-related kinases in the signaling pathway leading to the activation of IRF3 (3). However, we found that TRAF3 is not required for IL-1 to activate TBK1 and IKKε by the MyD88 pathway in fibroblasts (9), suggesting that TRAF3 may instead function "downstream" of, or in parallel with, the IKK-related kinases to couple TBK1 and IKKε to the phosphorylation of IRF3 by an unknown mechanism.

Materials and Methods

To measure the activity of the IKK-related kinases, endogenous TBK1 and IKKε were immunoprecipitated from 50 μg cell lysate protein using 1 μg of the corresponding sheep antibodies (TBK1-S041C; IKKε-S277C). Immunocomplexes were washed three times in lysis buffer, twice in 50 mM Tris-HCl pH 7.5, 0.1% (vol/vol) 2-mercaptoethanol, 0.1 mM EGTA, 10 mM magnesium acetate, and then resuspended in 25 μL of the same buffer containing 2 μM of recombinant GST-IRF3, 0.1 mM [γ-^{32}P]ATP (2,500 cpm/pmol). After incubation at 30 °C, reactions were terminated by the addition of 25 μL of 2% (wt/vol) SDS containing 40 mM EDTA pH 7.0, heated for 5 min at 100 °C, separated by SDS/PAGE, and the phosphorylated IRF3 was detected by autoradiography and quantitated by scanning using a phosphorimager. We validated this assay by demonstrating that activity in the TBK1 and IKKε immunoprecipitates was completely suppressed by MRT67307, a relatively specific inhibitor of the IKK-related kinases that does not affect the canonical IKKs (Fig. S1*A*) (9). This result shows that the activity being measured is TBK1 and IKKε and not another protein kinase(s) present in the immunoprecipitates as a contaminant. The activation of TBK1 and IKKε was also monitored in parallel by immunoblotting using a phospho-specific antibody that recognizes the activation loop residue Ser172 (9, 24).

ACKNOWLEDGMENTS. We thank Julia Carr and Gail Fraser for genotyping the mice, the University of Dundee Resource Centre (coordinated by Don Tennant and Lorraine Malone) for housing the mice, and the protein and antibody production teams of the Division of Signal Transduction Therapy, Medical Research Council (MRC) Protein Phosphorylation Unit, University of Dundee (coordinated by Hilary McLauchlan and James Hastie) for proteins and antibodies. K.C. was the recipient of a long-term fellowship from the European Molecular Biology Organization during part of this work. The work was supported by the UK MRC, AstraZeneca, Boehringer-Ingelheim, GlaxoSmithKline, Merck-Serono, and Pfizer.

1. Kawagoe T, et al. (2009) TANK is a negative regulator of Toll-like receptor signaling and is critical for the prevention of autoimmune nephritis. *Nat Immunol* 10:965–972.
2. Nanda SK, et al. (2011) Polyubiquitin binding to ABIN1 is required to prevent autoimmunity. *J Exp Med* 208:1215–1228.
3. Kawai T, Akira S (2010) The role of pattern-recognition receptors in innate immunity: Update on Toll-like receptors. *Nat Immunol* 11:373–384.
4. Kanayama A, et al. (2004) TAB2 and TAB3 activate the NF-kappaB pathway through binding to polyubiquitin chains. *Mol Cell* 15:535–548.
5. Wang C, et al. (2001) TAK1 is a ubiquitin-dependent kinase of MKK and IKK. *Nature* 412:346–351.
6. Ea CK, Deng L, Xia ZP, Pineda G, Chen ZJ (2006) Activation of IKK by TNFalpha requires site-specific ubiquitination of RIP1 and polyubiquitin binding by NEMO. *Mol Cell* 22:245–257.
7. Wu CJ, Conze DB, Li T, Srinivasula SM, Ashwell JD (2006) Sensing of Lys 63-linked polyubiquitination by NEMO is a key event in NF-kappaB activation [corrected]. *Nat Cell Biol* 8:398–406.
8. Xia ZP, et al. (2009) Direct activation of protein kinases by unanchored polyubiquitin chains. *Nature* 461:114–119.
9. Clark K, et al. (2011) Novel cross-talk within the IKK family controls innate immunity. *Biochem J* 434:93–104.
10. Beinke S, Robinson MJ, Hugunin M, Ley SC (2004) Lipopolysaccharide activation of the TPL-2/MEK/extracellular signal-regulated kinase mitogen-activated protein kinase cascade is regulated by IkappaB kinase-induced proteolysis of NF-kappaB1 p105. *Mol Cell Biol* 24:9658–9667.
11. Waterfield M, Jin W, Reiley W, Zhang M, Sun SC (2004) IkappaB kinase is an essential component of the Tpl2 signaling pathway. *Mol Cell Biol* 24:6040–6048.
12. Häcker H, Karin M (2006) Regulation and function of IKK and IKK-related kinases. *Sci STKE* 2006:re13.
13. Fitzgerald KA, et al. (2003) IKKepsilon and TBK1 are essential components of the IRF3 signaling pathway. *Nat Immunol* 4:491–496.
14. Sharma S, et al. (2003) Triggering the interferon antiviral response through an IKK-related pathway. *Science* 300:1148–1151.
15. Hemmi H, et al. (2004) The roles of two IkappaB kinase-related kinases in lipopolysaccharide and double stranded RNA signaling and viral infection. *J Exp Med* 199: 1641–1650.
16. Perry AK, Chow EK, Goodnough JB, Yeh WC, Cheng G (2004) Differential requirement for TANK-binding kinase-1 in type I interferon responses to toll-like receptor activation and viral infection. *J Exp Med* 199:1651–1658.
17. Pomerantz JL, Baltimore D (1999) NF-kappaB activation by a signaling complex containing TRAF2, TANK and TBK1, a novel IKK-related kinase. *EMBO J* 18:6694–6704.
18. Fujita F, et al. (2003) Identification of NAP1, a regulatory subunit of IkappaB kinase-related kinases that potentiates NF-kappaB signaling. *Mol Cell Biol* 23:7780–7793.
19. Ryzhakov G, Randow F (2007) SINTBAD, a novel component of innate antiviral immunity, shares a TBK1-binding domain with NAP1 and TANK. *EMBO J* 26:3180–3190.
20. Morton S, Hesson L, Peggie M, Cohen P (2008) Enhanced binding of TBK1 by an optineurin mutant that causes a familial form of primary open angle glaucoma. *FEBS Lett* 582:997–1002.
21. Chau TL, et al. (2008) Are the IKKs and IKK-related kinases TBK1 and IKK-epsilon similarly activated? *Trends Biochem Sci* 33:171–180.
22. Zhao T, et al. (2007) The NEMO adaptor bridges the nuclear factor-kappaB and interferon regulatory factor signaling pathways. *Nat Immunol* 8:592–600.
23. Chariot A, et al. (2002) Association of the adaptor TANK with the I kappa B kinase (IKK) regulator NEMO connects IKK complexes with IKK epsilon and TBK1 kinases. *J Biol Chem* 277:37029–37036.
24. Clark K, Plater L, Peggie M, Cohen P (2009) Use of the pharmacological inhibitor BX795 to study the regulation and physiological roles of TBK1 and IkappaB kinase epsilon: A distinct upstream kinase mediates Ser-172 phosphorylation and activation. *J Biol Chem* 284:14136–14146.
25. Shimada T, et al. (1999) IKK-i, a novel lipopolysaccharide-inducible kinase that is related to IkappaB kinases. *Int Immunol* 11:1357–1362.
26. Lang V, et al. (2003) betaTrCP-mediated proteolysis of NF-kappaB1 p105 requires phosphorylation of p105 serines 927 and 932. *Mol Cell Biol* 23:402–413.
27. Delhase M, Hayakawa M, Chen Y, Karin M (1999) Positive and negative regulation of IkappaB kinase activity through IKKbeta subunit phosphorylation. *Science* 284: 309–313.
28. Gatot JS, et al. (2007) Lipopolysaccharide-mediated interferon regulatory factor activation involves TBK1-IKKepsilon-dependent Lys(63)-linked polyubiquitination and phosphorylation of TANK/I-TRAF. *J Biol Chem* 282:31131–31146.
29. Bloor S, et al. (2008) Signal processing by its coil zipper domain activates IKK gamma. *Proc Natl Acad Sci USA* 105:1279–1284.
30. Cheng G, Baltimore D (1996) TANK, a co-inducer with TRAF2 of TNF- and CD 40L-mediated NF-kappaB activation. *Genes Dev* 10:963–973.
31. Rothe M, et al. (1996) I-TRAF is a novel TRAF-interacting protein that regulates TRAF-mediated signal transduction. *Proc Natl Acad Sci USA* 93:8241–8246.
32. Kagan JC, et al. (2008) TRAM couples endocytosis of Toll-like receptor 4 to the induction of interferon-beta. *Nat Immunol* 9:361–368.
33. Häcker H, et al. (2006) Specificity in Toll-like receptor signalling through distinct effector functions of TRAF3 and TRAF6. *Nature* 439:204–207.
34. Oganesyan G, et al. (2006) Critical role of TRAF3 in the Toll-like receptor-dependent and -independent antiviral response. *Nature* 439:208–211.

Immunity
Article

Antiviral Protein Viperin Promotes Toll-like Receptor 7- and Toll-like Receptor 9-Mediated Type I Interferon Production in Plasmacytoid Dendritic Cells

Tatsuya Saitoh,[1,2] Takashi Satoh,[1,2] Naoki Yamamoto,[3] Satoshi Uematsu,[1,2] Osamu Takeuchi,[1,2] Taro Kawai,[1,2] and Shizuo Akira[1,2,*]
[1]Laboratory of Host Defense, WPI Immunology Frontier Research Center, Osaka University, 3-1 Yamada-oka, Suita, Osaka 565-0871, Japan
[2]Department of Host Defense, Research Institute for Microbial Diseases, Osaka University, 3-1 Yamada-oka, Suita, Osaka 565-0871, Japan
[3]Department of Microbiology, Yong Loo Lin School of Medicine, National University of Singapore, Block MD4A, 5 Science Drive 2, 117597, Singapore
*Correspondence: sakira@biken.osaka-u.ac.jp
DOI 10.1016/j.immuni.2011.03.010

SUMMARY

Toll-like receptor 7 (TLR7) and TLR9 sense viral nucleic acids and induce production of type I interferon (IFN) by plasmacytoid dendritic cells (pDCs) to protect the host from virus infection. We showed that the IFN-inducible antiviral protein Viperin promoted TLR7- and TLR9-mediated production of type I IFN by pDCs. Viperin expression was potently induced after TLR7 or TLR9 stimulation and Viperin localized to the cytoplasmic lipid-enriched compartments, lipid bodies, in pDCs. Viperin interacted with the signal mediators IRAK1 and TRAF6 to recruit them to the lipid bodies and facilitated K63-linked ubiquitination of IRAK1 to induce the nuclear translocation of transcription factor IRF7. Loss of Viperin reduced TLR7- and TLR9-mediated production of type I IFN by pDCs. However, Viperin was dispensable for the production of type I IFN induced by intracellular nucleic acids. Thus, Viperin mediates its antiviral function via the regulation of the TLR7 and TLR9-IRAK1 signaling axis in pDCs.

INTRODUCTION

Innate immunity, the first line of host defense against infectious agents, is initiated after the recognition of components of pathogens by pattern-recognition receptors (PRRs) (Medzhitov, 2009; O'Neill and Bowie, 2010; Takeuchi and Akira, 2010). PRRs, such as the Toll-like receptor (TLR), RIG-I-like receptor (RLR), NOD-like receptor (NLR), and the C-type lectin family, drive the coordinated activation of signaling pathways to produce type I interferon (IFN), proinflammatory cytokines, and chemokines, resulting in the induction of host defense response (Medzhitov, 2009; O'Neill and Bowie, 2010; Takeuchi and Akira, 2010).

Production of type I IFN is induced after the detection of viral nucleic acids by PRRs and plays a central role in the establishment of an antiviral state (Medzhitov, 2009; O'Neill and Bowie, 2010; Takeuchi and Akira, 2010). RNA helicases RIG-I and MDA-5, known as RLRs, sense RNA of RNA viruses in the cytoplasm and activate transcription factors IRF3 and IRF7, which induce interferon stimulation responsive element-dependent transcription, resulting in the production of type I IFN (Yoneyama and Fujita, 2010). In contrast, stimulator of interferon genes (STING; also known as MPYS, MITA, or ERIS) mediate the activation of the IRF3-dependent innate immune response induced by a cyclic diadenosine monophosphate of *Listeria monocytogenes* and a double stranded (ds) DNA of DNA viruses (Ishikawa et al., 2009). The IRF3- and IRF7-dependent innate immune responses are also induced after TLR stimulation (Medzhitov, 2009; O'Neill and Bowie, 2010; Takeuchi and Akira, 2010). TLR3 and TLR4 induce IRF3- and IRF7-dependent production of type I IFN after the recognition of extracellular dsRNA and lipopolysaccharide (LPS), respectively (Kawai and Akira, 2010). Plasmacytoid dendritic cells (pDCs) produce a burst amount of type I IFN after the engagement of TLR7 and TLR9. TLR7 detects the single stranded (ss) RNA of RNA viruses and TLR9 detects unmethylated CpG DNA of DNA viruses (Blasius and Beutler, 2010). In pDCs, the engagement of TLR7 or TLR9 in lysosomes triggers the potent activation of IRF7 via kinases IRAK1 and IKKα, leading to the robust production of type I IFN (Blasius and Beutler, 2010).

Inflammatory cytokines and chemokines are also required for the host defense response (Medzhitov, 2009; O'Neill and Bowie, 2010; Takeuchi and Akira, 2010). The engagement of all TLR members and NOD1 and NOD2 triggers the production of proinflammatory cytokines and chemokines via the activation of the transcription factor NF-κB (Medzhitov, 2009; O'Neill and Bowie, 2010; Takeuchi and Akira, 2010). C-type lectins, such as Dectin-1, also mediate the production of inflammatory cytokines via the tyrosine kinase Syk-dependent pathway (Takeuchi and Akira, 2010). Inflammasomes, the caspase-1 containing complexes, induce the processing of pro-IL-1β and subsequent production of the inflammatory cytokine IL-1β after microbial infection (Schroder and Tschopp, 2010). The three types of recognized inflammasomes are: the AIM2 (absent in melanoma 2) inflammasome, activated by cytosolic microbial dsDNA; IPAF (Ice protease-activating factor), activated by bacterial flagellin; and NALP3 (NACHT, LRR, and PYD domains-containing protein 3), activated after damage in an organelle such as disrupted homeostasis of the Golgi apparatus by the M2 protein of influenza virus (Schroder and Tschopp, 2010; Ichinohe et al., 2010).

The IFN-inducible genes, which are upregulated after stimulation by IFNs and the engagement of PRRs, are critically involved in the host defense response against infectious agents (Honda et al., 2006). Targeted disruption of IRF3 and IRF7 and type I IFN receptors renders the host susceptible to viral infection, clearly indicating the importance of type I IFN in antiviral innate immunity (Honda et al., 2006). Although the mechanism underlying the direct elimination of viruses by IFN-inducible genes has been studied for some time, there are still IFN-inducible genes of unknown function in PRR-triggered signaling pathways. Therefore, clarification of the roles of IFN-inducible genes in the regulation of PRR-mediated innate immune responses is clearly important in order to understand host defense.

In the present study we focused on Viperin (also known as RSAD2, Vig1, or Cig5), which was originally identified as one of the inducible genes during infection with human cytomegalovirus (Chin and Cresswell, 2001). Viperin is also induced by type I IFN, type II IFN, LPS, and RNA viruses (Chin and Cresswell, 2001; Severa et al., 2006). Viperin localizes on the endoplasmic reticulum and Golgi apparatus and is transported to lipid-enriched compartments called lipid droplets (Chin and Cresswell, 2001; Hinson and Cresswell, 2009a; Hinson and Cresswell, 2009b). Viperin harbors an amphipathic α-helix domain at its N-terminus and functions by anchoring on a lipid layer via this domain (Hinson and Cresswell, 2009b). Viperin suppresses the replication of influenza virus by disrupting the lipid rafts (Wang et al., 2007). Viperin can also suppress the replication of other types of viruses probably by acting as a radical S-adenosylmethionine (SAM) enzyme (Jiang et al., 2008; Jiang et al., 2010; Duschene and Broderick, 2010; Shaveta et al., 2010). Recentstudies have revealed that Viperin is involved in the activation of NF-κB and AP-1 in T cells (Qiu et al., 2009). However, it is unknown whether Viperin is involved in the PRR-mediated innate immune response. Here, we examined the potential involvement of Viperin in PRR-induced production of type I IFN, inflammatory cytokines, and chemokines and showed Viperin is important in TLR7- and TLR9-mediated production of type I IFN by pDCs.

RESULTS

Viperin Expression Induced by Pathogens

We examined the expression of Viperin after the engagement of various types of PRRs. The engagement of TLR3 and that of TLR4 resulted in the induction of Viperin in peritoneal macrophages (Figure 1A). The engagement of TLR7 and that of TLR9 also resulted in the induction of Viperin in splenic pDCs (Figure 1B). However, ligands for TLR2 or TLR5 failed to trigger the induction of Viperin (Figure 1A). Curdlan and zymosan, ligands for C-type lectin Dectin-1, also failed to induce the expression of Viperin (Figure 1A). The activation of RLR- or STING-signaling pathway resulted in the induction of Viperin in GMCSF-induced DCs (Figures 1C and 1D). The expression of Viperin was also induced after infection by *Salmonella typhimurium*, which triggered both TLR- and NLR-dependent signals (Figure 1D). We examined whether the induction of Viperin was regulated by IRF3 and a related transcription factor IRF7 because IRF3 is able to induce the transcription of Viperin, and these transcription factors are activated by nucleic acids and LPS (Severa et al., 2006; Ishikawa et al., 2009; Kawai and Akira 2010; Yoneyama and Fujita, 2010). Upregulation of Viperin by the pathogens was disrupted in macrophages or GMCSF-induced DCs lacking both IRF3 and IRF7. (Figures 1A, 1C, and 1D). In pDCs, IRF7 is required for TLR7 and TLR9-mediated expression of Viperin (Figure 1B). These results indicated that various types of PRRs could trigger the induction of Viperin via the activation of IRF3 and IRF7 and suggested a potential involvement of Viperin in the regulation of the PRR-mediated innate immune response.

Viperin Facilitates TLR7/9-Dependent Production of Type I IFN

To investigate a role for Viperin in the PRR-mediated innate immune response, we generated Viperin-deficient (*Rsad2*$^{-/-}$) mice (Figure S1A available online). Successful targeted disruption of the Viperin gene locus was confirmed by Southern blotting analysis (Figure S1B). Neither Viperin mRNA nor Viperin protein was detected in *Rsad2*$^{-/-}$ embryonic fibroblasts (Figures S1C and S1D). *Rsad2*$^{-/-}$ mice were found at Mendelian ratios and grew normally (Figure S1E).

We then assessed whether Viperin regulates TLR-dependent production of type I IFN. The production of type I IFN after the engagement of TLR7 with heat-treated Newcastle disease virus (NDV) or TLR9 by CpG DNA was impaired in *Rsad2*$^{-/-}$ FLT3L-induced DCs (Figures 2A and 2B). CpG DNA-induced IFN-β mRNA synthesis was attenuated in *Rsad2*$^{-/-}$ FLT3L-induced DCs, indicating that IFN-β production is reduced at the transcriptional level (Figure 2C). Viperin deficiency reduced the amount of intracellular IFN-α protein in B220^{+} FLT3L-induced DCs (Figure 2D). Consistent with these results, the production of IFN-α induced by A- and D-type CpG DNA was impaired in *Rsad2*$^{-/-}$ splenic pDCs, and the amount of IFN-α in the serum was reduced in *Rsad2*$^{-/-}$ mice injected with A- or D-type CpG DNA (Figures 2E and 2F). These results indicated that Viperin promotes TLR7 and TLR9-dependent production of type I IFN by pDCs. However, Viperin was not involved in the production of IL-12 p40 after TLR7 or TLR9 stimulation, suggesting a selective requirement of Viperin in the TLR7 and TLR9-mediated signaling pathway (Figures 2A–2C, 2E, and 2F). Complementation of wild-type Viperin, but not the N-terminal deletion mutant, into *Rsad2*$^{-/-}$ FLT3L-DCs restored IFN-β production induced by TLR7 or TLR9 engagement (Figure 2G). Because the N terminus of the Viperin protein is an amphipathic α-helix responsible for membrane association, anchoring on the membrane compartments is required for its function in the TLR7- or TLR9-mediated innate immune response. Viperin was dispensable for the TLR4-mediated IFN response because *Rsad2*$^{-/-}$ GMCSF-induced DCs produced normal amounts of IFN-β and CXCL10, an IFN-inducible chemokine, in response to LPS (Figure 2H).

We also assessed the involvement of Viperin in the production of type I IFN induced by intracellular nucleic acids. The production of type I IFN induced by transfected dsRNA or dsDNA was also normal in *Rsad2*$^{-/-}$ MEFs (Figure S2A). Viperin was dispensable for the production of type I IFN induced by NDV, encephalomyocarditis virus (EMCV), *L. monocytogenes*, or herpes simplex virus 1 (HSV1) (Figures S2B and S2C). These results indicated that Viperin does not regulate RLR- and STING-mediated IFN-β production.

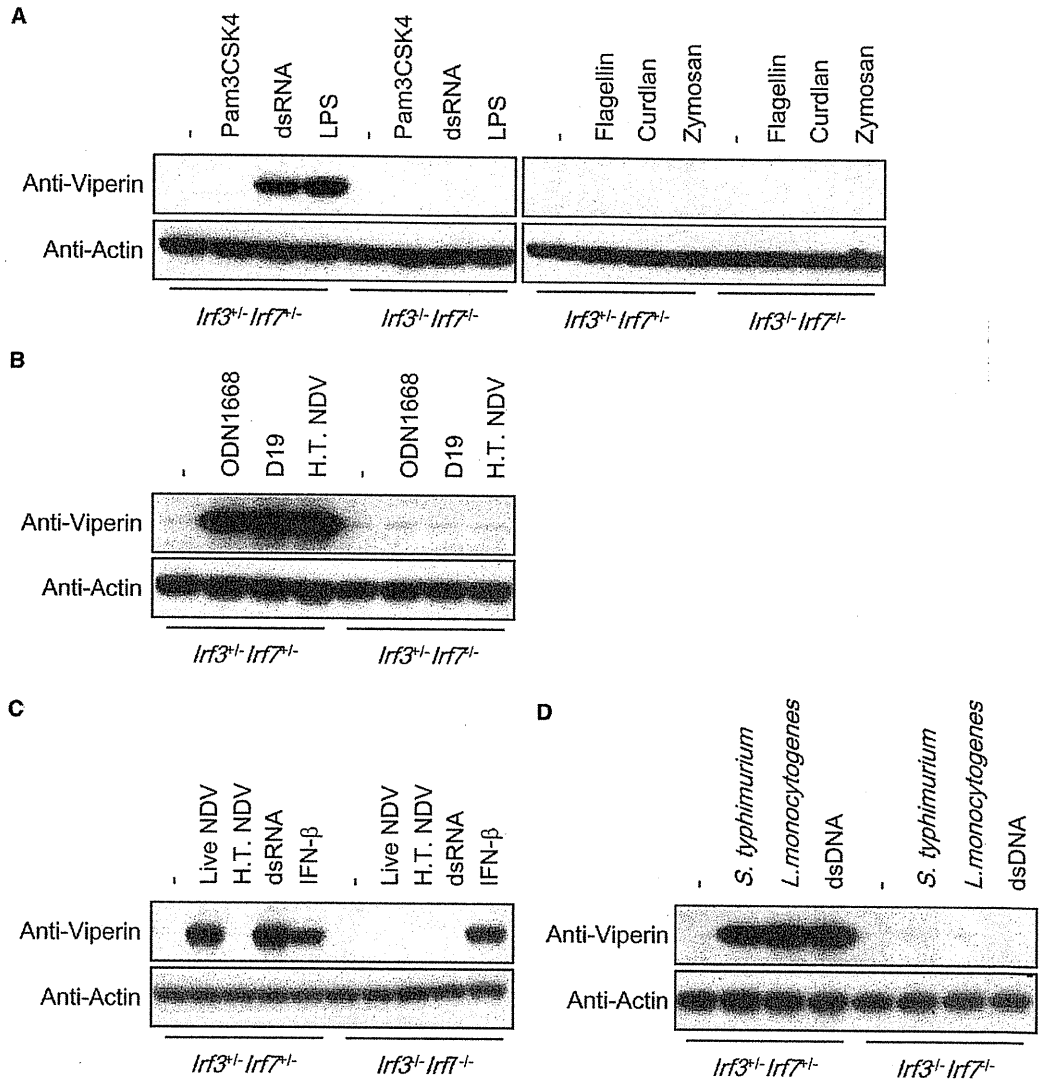

Figure 1. Induction of Viperin after Sensing of Pathogens

(A) Peritoneal macrophages from *Irf3*$^{+/-}$*Irf7*$^{+/-}$ and *Irf3*$^{-/-}$*Irf7*$^{-/-}$ mice were stimulated with the indicated ligands for 5 hr. Whole-cell lysate was subjected to immunoblotting analysis with the indicated antibodies.

(B) Splenic plasmacytoid dendritic cells from *Irf3*$^{+/-}$*Irf7*$^{+/-}$ and *Irf3*$^{+/-}$*Irf7*$^{-/-}$ mice were stimulated with indicated ligands for 5 hr.

(C) GMCSF-induced bone marrow dendritic cells from *Irf3*$^{+/-}$*Irf7*$^{+/-}$ and *Irf3*$^{-/-}$*Irf7*$^{-/-}$ mice were infected with live Newcastle disease virus (NDV) at a multiplicity of infection (MOI) equal to one or heat-treated (H.T.) NDV for 24 hr or were stimulated with dsRNA (poly rI-rC) plus LF2000 or IFN-β for 8 hr.

(D) Peritoneal macrophages from *Irf3*$^{+/-}$*Irf7*$^{+/-}$ and *Irf3*$^{-/-}$*Irf7*$^{-/-}$ mice were infected with *S. typhimurium* (MOI = 0.1) or *L. monocytogenes* (MOI = 20) for 24 hr or were stimulated with dsDNA (poly dA-dT) plus LF2000 for 8 hr. Data are representative of two independent experiments.

We next examined the involvement of Viperin in PRR-induced production of inflammatory cytokines. *Rsad2*$^{-/-}$ macrophages produced a normal amount of TNF and IL-6 after the engagement of TLR2, TLR4, TLR7, or TLR9 (Figure S2D). Viperin was also dispensable for the production of TNF and IL-1β after the engagement of Dectin-1 (Figure S2E). Viperin deficiency did not affect the production of IL-1β by the activation of the AIM2-, IPAF-, or NALP3 inflammasome (Figures S2F and S2G). Viperin was not involved in the enhancement of IL-6 production induced by the engagement of NOD1 or NOD2 (Figure S2H). These results indicated that Viperin does not regulate the production of inflammatory cytokines.

Interaction of Viperin with IRAK1 and TRAF6

Specific involvement of Viperin in TLR7 or TLR9-dependent type I IFN production prompted us to examine the molecular function of Viperin. The population of *Rsad2*$^{-/-}$ B220^{+}CD11C^{+} cells (generally regarded as pDCs; Blasius and Beutler, 2010; Kawai and Akira, 2010) was normal in splenocytes and in FLT3L-induced bone-marrow-derived cells, indicating that Viperin is

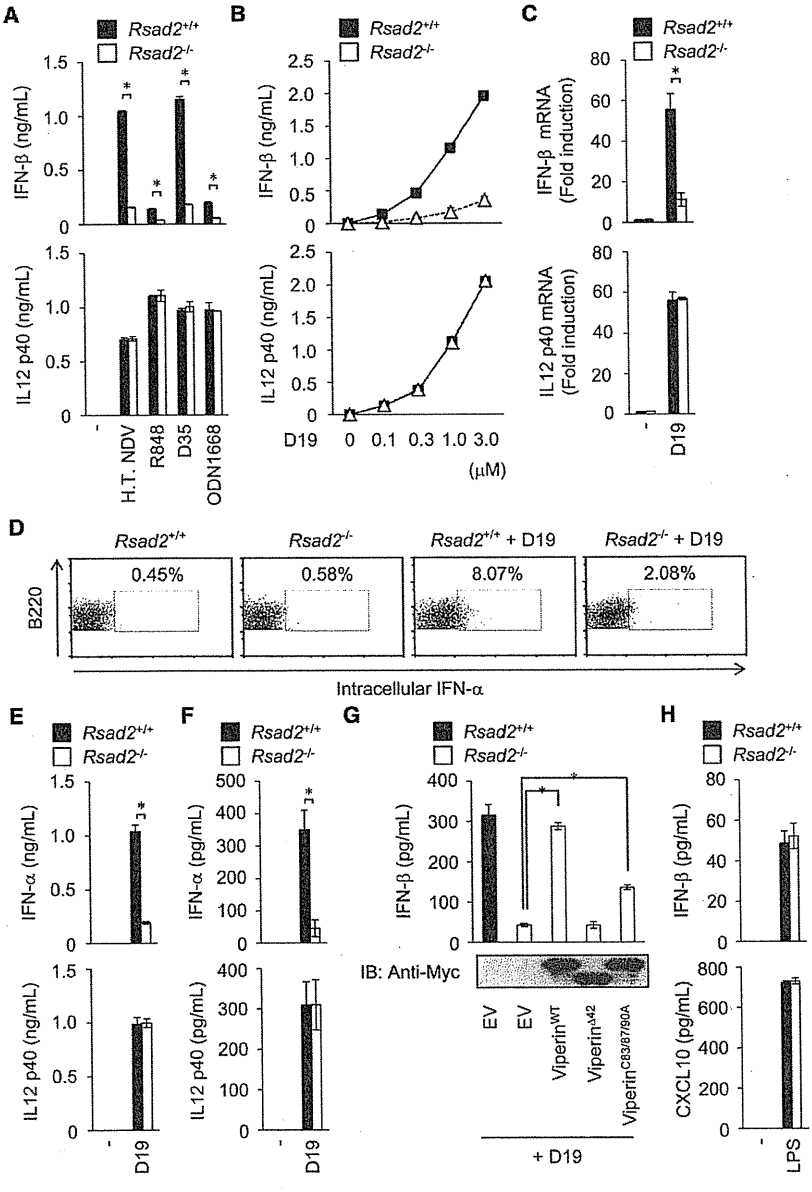

Figure 2. Viperin Promotes TLR7 and TLR9-Dependent Production of Type I IFNs by Plasmacytoid Dendritic Cells

(A and B) *Rsad2*$^{+/+}$ or *Rsad2*$^{-/-}$ FLT3L-induced bone marrow dendritic cells were stimulated with TLR7 ligands (H.T. NDV and R848) or TLR9 ligands (D19, D35 and ODN1668). Culture supernatant was collected 24 hr after stimulation and subjected to ELISA. The results shown are mean ± SD (n = 3). Statistical significance (p value) was determined by the Student's t test. *p < 0.01 (C) *Rsad2*$^{+/+}$ or *Rsad2*$^{-/-}$ FLT3L-induced bone-marrow dendritic cells were stimulated with D19 (1 μM) for 8 hr. Total RNA was isolated and subjected to quantitative RT-PCR analysis for IFN-β and IL-12 p40.

(D) Intracellular IFN-α staining of Flt3L-induced B220^{+} dendritic cells derived from *Rsad2*$^{+/+}$ or *Rsad2*$^{-/-}$ mice. The D19-stimulated cells were stained with anti-B220 and anti-IFN-α and were subjected to flow cytometry analysis.

(E) *Rsad2*$^{+/+}$ or *Rsad2*$^{-/-}$ splenic plasmacytoid dendritic cells were stimulated with D19 for 24 hr.

(F) *Rsad*$^{+/+}$ or *Rsad2*$^{-/-}$ mice were intravenously injected with D19 for the indicated time periods. The collected serum was subjected to ELISA.

(G) Viperin$^{wild\text{-}type}$, Viperin$^{\Delta 42}$, or Viperin$^{C83/87/90A}$ protein was expressed in bone marrow cells isolated from *Rsad2*$^{-/-}$ mice. The transduced cells were cultured in the presence of FLT3L for 7 days and then stimulated with D19 (1 μM) for 24 hr. Culture supernatant and whole-cell lysate were subjected to ELISA and immunoblotting analysis respectively.

(H) *Rsad2*$^{+/+}$ or *Rsad2*$^{-/-}$ GMCSF-induced bone marrow dendritic cells were stimulated with LPS (100 ng/mL) for 24 hr, and the culture supernatant was subjected to ELISA. Data are representative of three independent experiments.

not necessary for the development of pDCs (Figures S3A and S3B). Viperin does not regulate uptake of A- or D-type CpG DNA because the population positive for the FITC-labeled CpG DNA in *Rsad2*$^{-/-}$ B220^{+}CD11C^{+} DCs was comparable to that in wild-type DCs (Figure S3C). The expression level of LC3-I and LCII protein and p62 protein was not altered by Viperin deficiency (Figure S3D), indicating that Viperin does not regulate basal autophagy, which is required for the recognition of the viral genome by TLR7 and TLR9 in pDCs (Lee et al., 2007).

Because Viperin anchors on the cytoplasmic face of a lipid layer of the membrane compartments, we examined whether Viperin regulates essential signal mediators, such as IKKα, IRAK1, IRAK4, IRF7, MyD88, TRAF3, and TRAF6 (Kawai et al., 2004; Honda et al., 2004; Uematsu et al., 2005; Hoshino et al., 2006; Häcker et al., 2006). Viperin is dispensable for A- and D-type CpG DNA-induced phosphorylation of Ser176 and Ser180 residues of IKKα, which is an essential step for IFN response by pDCs (Figure S3E) (Gotoh et al., 2010). In conventional dendritic cells (cDCs), B- and K-type CpG DNA, but not A- and D-type CpG DNA, induces activation of the IKKα-IRF1 signaling axis leading to IFN-β production (Hoshino et al., 2010). Viperin was also dispensable for IKKα-mediated production of IFN-β induced by B- and K-type CpG DNA in cDCs (Figure S3F). These results indicated that Viperin does not regulate the activation of IKKα. We assessed the interaction of Viperin with the remaining essential mediators. When transiently expressed in 293 cells, IRAK1 and TRAF6 interacted with Viperin, whereas the other mediators, IRAK4, IRF7, MyD88, and TRAF3, appeared not to interact with Viperin (Figures 3A and 3B). In FLT3-induced DCs stimulated with A- andD-type CpG DNA, endogenous Viperin interacted with endogenous IRAK1 and endogenous TRAF6 (Figures 3C and 3D). When ectopically expressed, Viperin$^{\Delta 42}$